A synthesis of ocean total alkalinity and dissolved inorganic carbon measurements from 1993 to 2022: the SNAPO-CO2-v1 dataset

Nicolas Metzl[1], Jonathan Fin[1,2], Claire Lo Monaco[1], Claude Mignon[1], Samir Alliouane[3], David Antoine[3,4], Guillaume Bourdin[5], Jacqueline Boutin[1], Yann Bozec[6], Pascal Conan[7,8], Laurent Coppola[3,8], Frédéric Diaz[*], Eric Douville[9], Xavier Durrieu de Madron[10], Jean-Pierre Gattuso[3,11], Frédéric Gazeau[3], Melek Golbol[8,12], Bruno Lansard[9], Dominique Lefèvre[13], Nathalie Lefèvre[1], Fabien Lombard[3,14], Férial Louanchi[15], Liliane Merlivat[1], Léa Olivier[1,16], Anne Petrenko[13], Sébastien Petton[17], Mireille Pujo-Pay[7], Christophe Rabouille[9], Gilles Reverdin[1], Céline Ridame[1], Aline Tribollet[1], Vincenzo Vellucci[8,12], Thibaut Wagener[13], Cathy Wimart-Rousseau[13,18]

[1] Laboratoire LOCEAN/IPSL, Sorbonne Université-CNRS-IRD-MNHN, Paris, 75005, France
[2] OSU Ecce Terra, Sorbonne Université-CNRS, Paris, 75005, France
[3] Sorbonne Université, CNRS, Laboratoire d'Océanographie de Villefranche, LOV, F-06230 Villefranche-sur-Mer, France
[4] Remote Sensing and Satellite Research Group, School of Earth and Planetary Sciences, Curtin University, Perth WA 6845, Australia
[5] School of Marine Sciences, University of Maine, Orono, USA
[6] Station Biologique de Roscoff, UMR 7144 – EDYCO-CHIMAR, Roscoff, France
[7] Sorbonne Université, CNRS, Laboratoire d'Océanographie Microbienne, LOMIC, F-66650 Banyuls-sur-Mer, France
[8] Sorbonne Université, CNRS, OSU Station Marines, STAMAR, Paris, F-75006, France
[9] Laboratoire des Sciences du Climat et de l'Environnement, LSCE/IPSL, UMR 8212 CEA- CNRS-UVSQ, Université Paris-Saclay, 91191 Gif-sur-Yvette, France
[10] CEFREM, CNRS-Université de Perpignan Via Domitia, 52 Avenue Paul Alduy, 66860 Perpignan, France
[11] Institute for Sustainable Development and International Relations, Sciences Po, 27 rue Saint Guillaume, F-75007 Paris, France
[12] Sorbonne Université, CNRS, Institut de la Mer de Villefranche, IMEV, Villefranche-sur-Mer, F-06230, France
[13] Aix Marseille Univ, Université de Toulon, CNRS, IRD, MIO, Marseille, France
[14] Research Federation for the study of Global Ocean Systems Ecology and Evolution, FR2022/Tara GOSEE, 75000, Paris, France.
[15] CVRM: Laboratoire de Conservation et de Valorisation des Ressources Marines, Ecole Nationale Supérieure des Sciences de la Mer et de l'Aménagement du Littoral (ENSSMAL), Station de recherche de Sidi Fredj, Algeria
[16] Alfred Wegener Institute, Helmholtz Centre for Polar and Marine Research, Bremerhaven, Germany
[17] Ifremer, Univ Brest, CNRS, IRD, LEMAR, F-29840 Argenton, France
[18] GEOMAR Helmholtz Centre for Ocean Research Kiel, 24105 Kiel, Germany
* Passed away 14/3/2021

Correspondence to: Nicolas Metzl (nicolas.metzl@locean.ipsl.fr)

Abstract. Total alkalinity (A_T) and dissolved inorganic carbon (C_T) in the oceans are important properties to understand the ocean carbon cycle and its link with global change (ocean carbon sinks and sources, ocean acidification) and ultimately find carbon based solutions or mitigation procedures (marine carbon removal). We present a database of more than 44 400 A_T and C_T observations along with basic ancillary data (time and space location, depth, temperature and salinity) in various ocean regions obtained since 1993 mainly in the frame of French projects. This includes both surface and water columns data acquired in open oceans, coastal zones and in the Mediterranean Sea and either from time-series or punctual cruises. Most A_T and C_T data in this synthesis were measured from discrete samples using the same closed-cell potentiometric titration calibrated with Certified

Reference Material, with an overall accuracy of ± 4 µmol kg^{-1} for both A_T and C_T. The data are provided in two separate datasets for the global ocean, and for the Mediterranean Sea (https://doi.org/10.17882/95414, Metzl et al., 2023) that offers a direct use for regional or global purposes, e.g. A_T/Salinity relationships, long-term C_T estimates, constraint and validation of diagnostics C_T and A_T reconstructed fields or ocean carbon and coupled climate/carbon models simulations, as well as data derived from Biogeochemical-Argo (BGC-Argo) floats. When associated with other properties, these data can also be used to calculate pH, fugacity of CO_2 (fCO_2) and other carbon system properties to derive ocean acidification rates or air-sea CO_2 fluxes.

1 Introduction

Since 1750, humans activities have added 700 (±75) PgC anthropogenic carbon dioxide to the atmosphere by burning fossil fuels, producing cement and changing land use (Friedlingstein et al., 2022) driving up the atmospheric carbon dioxide (CO_2) level and leading to unequivocal global change. The ocean plays a major role in reducing the impact of climate change by absorbing more than 90% of the excess heat in the climate system (Cheng et al., 2020; von Schuckmann et al, 2020, 2023; IPCC, 2022) and about 25% of human released CO_2 (Friedlingstein et al., 2022). However, the oceanic CO_2 uptake changes the chemistry of seawater reducing its buffering capacity (Revelle and Suess, 1957; Jiang et al, 2023a) and leading to a process known as ocean acidification with potential impacts on marine organisms (Fabry et al., 2008; Doney et al., 2009, 2020; Gattuso et al., 2015). With atmospheric CO_2 concentrations, surface ocean temperature and ocean heat content, sea-level, sea-ice and glaciers, the ocean acidification (decrease of pH) is now recognized by the World Meteorological Organization as one of the 7 key properties for global climate indicators (WMO, 2018). In the frame of the 2030 Agenda, the United Nations established a set of Sustainable Development Goals (SDG; United Nations, 2020), including a goal dedicated to the ocean (SDG 14, “Life below water”) which calls to "conserve and sustainably use the oceans, seas and marine resources for sustainable development". Ocean acidification is specifically referred in the SDG indicator 14.3.1 coordinated at the Intergovernmental Oceanographic Commission (IOC) of UNESCO. Observing the carbonate system in the oceans and marginal seas and understanding how this system changes over time is thus highly relevant not only to quantify the global ocean carbon budget, the anthropogenic CO_2 inventories or ocean acidification rates, but also to understand and simulate the processes that govern the complex CO_2 cycle in the ocean and to better predict the future evolution of climate and global changes (Eyring et al., 2016; Kwiatkowski et al., 2020; Jiang et al., 2023a).

The number and quality of ocean fCO_2, A_T, C_T and pH measurements have increased substantially over the past few decades. Quality-controlled observations are now regularly assembled in global data syntheses such as SOCAT (Surface Ocean CO_2 Atlas, Pfeil et al., 2013; Bakker et al., 2014, 2016) and GLODAP (Global Ocean Data Analysis Project, Key et al., 2004; Olsen et al., 2016, 2019, 2020; Lauvset et al., 2021, 2022). These datasets allow evaluation of properties trends in the global ocean, including the change of the ocean CO_2 sink (e.g. Wanninkhof et al., 2013; Friedlingstein et al., 2022; Watson et al., 2020), anthropogenic CO_2 inventories (e.g. Sabine et al., 2004; Khatiwala et al., 2013; Gruber et al., 2019) and ocean acidification (Lauvset et al., 2015, 2020; Jiang et al., 2019; Feely et al, 2023; Ma et al, 2023). Thanks to publicly available consistent and quality controlled databases new methods were recently developed (Carter et al, 2016; Sauzède et al., 2017; Bittig et al., 2018) to reproduce A_T and C_T distributions from other properties like temperature, salinity and oxygen more often observed in the water column especially from autonomous floats (Claustre et al., 2020; Mignot et al., 2023). These methods (named CANYON-B and CONTENT, Bittig et al., 2018) are now also used

to help decisions on GLODAP data quality control or to fill in observational gaps (Olsen et al., 2019, 2020; Tanhua et al., 2019, 2021). The GLODAP data products were also successfully used to construct new global ocean A_T and C_T climatological monthly fields in surface and water column using neural network method (e.g. Broullón et al., 2019, 2020).

Following pioneer works that produced various global-ocean climatologies of the sea-surface carbonate system (Millero et al., 1998; Lee et al., 2000, 2006; Takahashi et al., 2002, 2009, 2014; Sasse et al., 2013; Jiang et al., 2019), the coupling of fCO_2 data (from SOCAT) and A_T data (from GLODAP) now enables reconstruction of the full carbonate system in the surface ocean at monthly scale to investigate temporal trends at decadal scale (e.g. Gregor and Gruber, 2021; Keppler et al., 2023).

International projects such as SOCAT and GLODAP offer important way to synthetize ocean carbon data. In these projects, each observation is quality controlled offering to users high quality observations for regional or global analysis, either for processes analysis or to constraint or validate of ocean and coupled climate/carbon models (CMIP6, e.g. Lerner et al., 2021). SOCAT is a publicly available synthesis product initiated in 2007 (Metzl et al., 2007) for quality-controlled, surface ocean fCO_2 (fugacity of carbon dioxide) observations made by the international marine carbon research community (Bakker et al., 2016). The first SOCAT version was released in 2011 (Pfeil et al., 2013; Sabine et al., 2013), followed by 6 SOCAT versions (Bakker et al., 2014, 2016). The last version in 2023 includes more than 40 million fCO_2 data with accuracy better than 5 µatm (Bakker et al., 2023). One important product from SOCAT is the use of data to estimate global air-sea CO_2 fluxes based on reconstructed pCO_2 fields (e.g. Surface Ocean pCO_2 Mapping Intercomparison, SOCOM, Rödenbeck et al., 2015). Since 2015, these results are included each year for the global carbon budget (Le Quere et al., 2015; Friedlingstein et al., 2022).

On the other hand, following WOCE/JGOFS era in the 90s when almost all observations were started to be synthetized in a specific recommended format (Joyce and Corry, 1994), GLODAP focusses on water-column carbon observations (and other properties). Following the original GLODAP data product (Key et al., 2004), the project accumulated many new quality controlled observations. One important achievement from GLODAP is the use of data to estimate the anthropogenic CO_2 inventory or its change over decades (Sabine et al., 2004; Gruber et al., 2019). Both products, SOCAT and GLODAP, are relevant tools to detect oceanic acidification rates (Lauvset et al., 2015; Jiang et al., 2019; Feely et al, 2023; Ma et al, 2023).

Although these projects include many international ocean observations there are ocean CO_2 related observations all around the world (published or not published), such as total alkalinity and dissolved inorganic carbon, that are not included in SOCAT or GLODAP. This is because SOCAT accepts and controls only fCO_2 data, whereas GLODAP includes and controls water-columns data mainly from WOCE/GO-SHIP/CLIVAR cruises. It should be noticed that many ocean carbon observations in various formats can be also found in dedicated database such as NCEI/OCADS (former CDIAC-Ocean, Jiang et al., 2023b, https://www.ncei.noaa.gov/products/ocean-carbon-acidification-data-system), PANGAEA (https://www.pangaea.de/) or Seanoe (https://www.seanoe.org/). In this context it is recommended to progress in data synthesis of the ocean carbon observations that would offer new high quality products for the community (e.g. for GOA-ON, www.goa-on.org, IOC/SDG 14.1.3, https://oa.iode.org/, Tilbrook et al., 2019).

In this work, we present a synthesis of more than 44 400 A_T and C_T observations obtained over the 1993-2022 period during various cruises or at time-series stations mainly supported by French projects. This dataset merges observations measured with the same instruments thus being analytically coherent. Most of the data have accuracy better than ±4 µmol kg^{-1}, i.e. between the climate (±2 µmol kg^{-1}) and weather (±10 µmol kg^{-}

[1]) goals (Newton et al, 2015; Bockmon and Dickson, 2015). Hereafter this dataset will be cited as SNAPO-CO2-V1. We describe the data assemblage and associated quality control and discuss some potential uses of this dataset.

2 Data collections

The time series projects and research cruises from which data were collated are listed in Table 1 with references in the Supplementary file (Table S1) and the sampling locations displayed in Figure 1. Sampling was performed either from CTD-Rosette casts (Niskin bottles) or from the ship's seawater supply (intake at about 5m depth depending the ship and swell). Samples collected in 500 mL borosilicate glass bottles were poisoned with 100 to 300 µL of $HgCl_2$ depending on the cruises, closed with greased stoppers (Apiezon®) and held tight using elastic band following the SOP protocol (Dickson et al., 2007). Some samples were also collected in 500 mL bottles closed with screw caps. After completion of each cruise, discrete samples were returned back to the LOCEAN laboratory (Paris, France) and stored in a dark room at 4 °C before analysis generally within 2-3 months after sampling (sometimes within a week). Some samples were also measured for specific processes studies on benthic corals (e.g. Maier et al., 2012; McCulloch et al., 2012) or for mesocosm and culture experiments but the data are not included in this synthesis as they do not represent natural ocean state (e.g. addition of Sahara dust during the DUNE project, Ridame et al., 2014).

As opposed to pCO_2, surface A_T or C_T observations are generally obtained from discrete sampling (measured onboard or onshore). Few cruises offer sea-surface semi-continuous A_T or C_T observations (e.g. Metzl et al., 2006) but new instrumental developments (Seelmann et al., 2020) now enable A_T measurements on Ship of Opportunity Program lines (SOOP). In addition to discrete samples analyzed for various projects conducted mainly in the North Atlantic, Tropical Atlantic, Tropical Pacific, Mediterranean sea and coastal regions (Table 1), we complemented this synthesis with A_T and C_T surface observations obtained in the Indian and Southern oceans during the OISO cruises in 1998-2018 (Metzl et al., 2006; Leseurre et al., 2022; data also available at NCEI/OCADS: www.nodc.noaa.gov/ocads/oceans/VOS_Program/OISO.html) and the recent CLIM-EPARSES cruise conducted in the Mozambique Channel in April 2019 (Lo Monaco et al., 2020, 2021). For OISO cruises the water-column observations are part of the CARINA (CARbon IN the Atlantic) and GLODAP synthesis products (Lo Monaco et al., 2010; Olsen et al., 2016, 2019, 2020) and not included here. Excepted when specified, all data in this synthesis were obtained using the same technique used either in laboratory or at sea (for OISO 1998-2018 and CLIM-EPARSES 2019 cruises).

Table 1: List of cruises in the SNAPO-CO2-v1 dataset. This is organized by region: Global Ocean and coastal zones, and Mediterranean Sea (MedSea). See Tables S1, S2, S4 and S4 in the Supplementary Material for a list of laboratories, of CRMs used, for references and for DOI of cruises. Nb = the number of data for each cruise or time-series. * indicates the measurements at sea (surface underway)

Cruise/Project	Start	End	Region	Sampling	Nb
AWIPEV	2015	2021	Arctic	Surface and sub-surface	195
SURATLANT+RREX	1993	2017	North Atlantic	Surface	2832
OVIDE	2006	2018	North Atlantic	Surface, Water Column	397
STRASSE	2012		North Atlantic	Water Column	205
EUREC4A-OA	2020		North Atlantic	Surface, Water Column	135
PROTEUS	2010		North Atlantic	Water Column	27
CHANNEL	2012	2015	English Channel	Surface	696
SOMLIT-Brest	2008	2019	Coastal North Atl	Surface	1174
SOMLIT-Roscoff	2009	2019	Coastal North Atl	Surface and 60m	801
ECOSCOPA	2017	2019	Coastal North Atl	Surface	67
PENZE	2011	2020	River Brittany	Surface and sub-surface	148
AULNE	2009	2010	River Brittany	Surface	27
ELORN	2009	2009	River Brittany	Surface	28
BIOZAIRE	2003	2004	Trop Atlantic	Water Column	87
EGEE	2005	2007	Trop Atlantic	Surface	199
PIRATA-FR	2009	2017	Trop Atlantic	Surface, Water Column	513
PLUMAND	2007		Trop Atlantic	Surface	38
OUTPACE	2015		Trop Pacific	Water Column	240
PANDORA	2012		Solomon Sea	Water Column	178
TARA-Pacific	2016	2018	Trop Pac North Atl	Surface and sub-surface	325
TARA-Ocean	2009	2012	Global Ocean	Surface + 400m	123
TARA-Microbiome	2021	2022	Atlantic	Surface, Water Column	216
ACE	2016	2017	Southern Ocean	Surface, Water Column	135
MOBYDICK	2019		Southern Ocean	Water Column	64
CLIM-EPARSES *	2019		Indian	Surface	790
OISO *	1998	2018	South Indian	Surface	24950
DYFAMED	1998	2017	MedSea	Water Column	2118
BOUSSOLE	2014	2019	MedSea	Surface + 10m	172
SOMLIT-PointB	2007	2015	MedSea Coastal	Surface + 50m	2397
ANTARES	2010	2016	MedSea	Water Column	502
MOLA	2010	2013	MedSea Coastal	Water Column	66
SOLEMIO	2016	2018	MedSea Coastal	Water Column	212
MOOSE-GE	2010	2019	MedSea	Water Column	1847
LATEX	2010		MedSea	Water Column	51
CARBORHONE	2011	2012	MedSea	Water Column	706
CASCADE	2011		MedSea	Water Column	218
DEWEX	2013		MedSea	Water Column	367
SOMBA	2014	2014	MedSea	Water Column	203
AMOR-BFLUX	2015		MedSea Coastal	Water Column	6
PEACETIME	2017	2017	MedSea	Water Column	233
PERLE	2018	2021	MedSea	Water Column	805

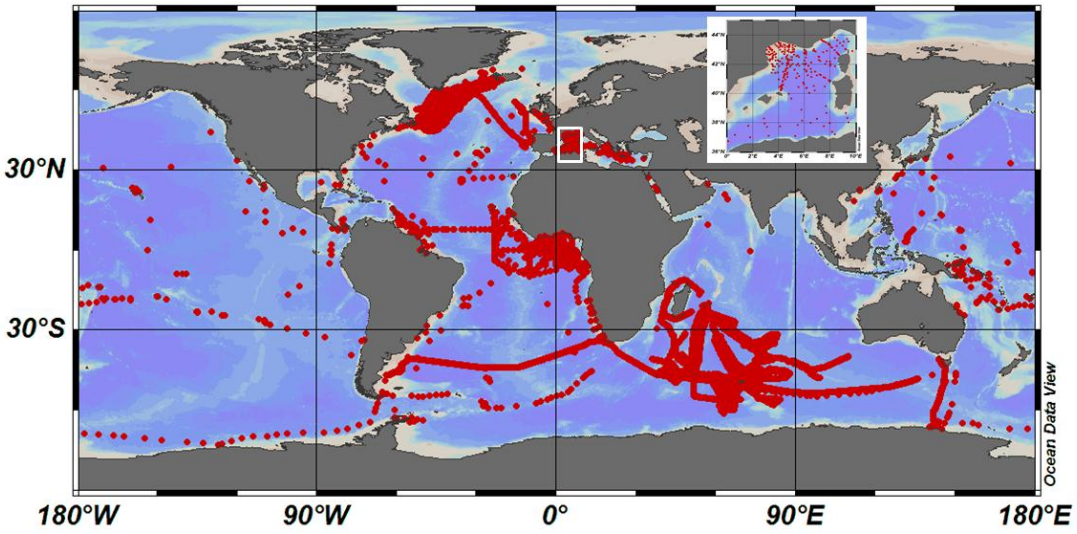

Figure 1: Locations of A_T and C_T data (1993-2022) in the Global Ocean and the Western Mediterranean Sea (white box, insert) in the SNAPO-CO2-v1 dataset. Figure produced with ODV (Schlitzer, 2018).

3 Method, accuracy, repeatability, inter-comparison and quality control

3.1 Method and accuracy

Since 2003, the discrete samples returned back at SNAPO-CO2 Service facilities (LOCEAN, Paris), were analyzed simultaneously for A_T and C_T by potentiometric titration using a closed cell (Edmond, 1970; Goyet et al., 1991). The same technique was used at sea for surface water underway measurements during OISO and CLIM-EPARSES cruises (indicated by * in Table 1). For two time series, the dataset also includes measurements obtained before 2000 using other techniques: the DYFAMED time-series observations measured between in 1998 and 2000 in the Mediterranean Sea (Copin-Montégut and Bégovic, 2002; Coppola et al., 2020) and the SURATLANT time-series values acquired from 1993 to 1997 in the North Atlantic subpolar gyre (Reverdin et al., 2018). We also include A_T data in the river Penzé (Brittany) in 2019-2020 (Yann Bozec, SBR/Roscoff, pers. comm.).

In the late 1980s the so-called "JGOFS-IOC Advisory Panel on Ocean CO2" recommended the need for standard analysis protocols and for developing Certified Reference Materials (CRMs) for inorganic carbon measurements (Poisson et al., 1990; UNESCO, 1990, 1991). The CRMs were provided to international laboratories by Pr. A. Dickson (Scripps Institution of Oceanography, San Diego, USA), starting in 1990 for C_T and 1996 for A_T, respectively. These CRMs were thus always available to us and used to calibrate the measurements (CRM Batch numbers used for each cruise are listed in Supplementary file (Table S2). The concentrations of CRMs we used vary between 2193 and 2426 µmol kg^{-1} for A_T and between 1968 and 2115 µmol kg^{-1} for C_T corresponding to the range of concentrations observed in open ocean water. The CRMs accuracy, as indicated in the certificate for each Batch, is around ±0.5 µmol kg^{-1} for both A_T and C_T (www.nodc.noaa.gov/ocads/oceans/Dickson_CRM/batches.html).

Results of analyses performed on 965 CRM bottles (different Batches) in 2013-2023 are presented in Figure 2. The standard-deviations of the differences of measurements were on average around ±3.5 µmol kg^{-1} for

both A_T and C_T. For unknown reasons, the differences were occasionally up to 10-15 µmol kg^{-1} (0.8% of the data, Figure S2). These few CRM measurements were discarded for the data processing. On average, and excluding some outliers, standard-deviations of the differences for 1090 CRM analyses were ±2.71 µmol kg^{-1} for A_T and ±2.86 µmol kg^{-1} for C_T, respectively. We did not detect any specific signal for CRM analyses (e.g., larger uncertainty depending on the Batch number or temporal drifts during analyses, Figure 2) but for some cruises the accuracy based on CRMs could be slightly better than 3 µmol kg^{-1} (e.g. Marrec et al., 2014: Touratier et al., 2016; Ganachaud et al., 2017; Wimart-Rousseau et al., 2020a).

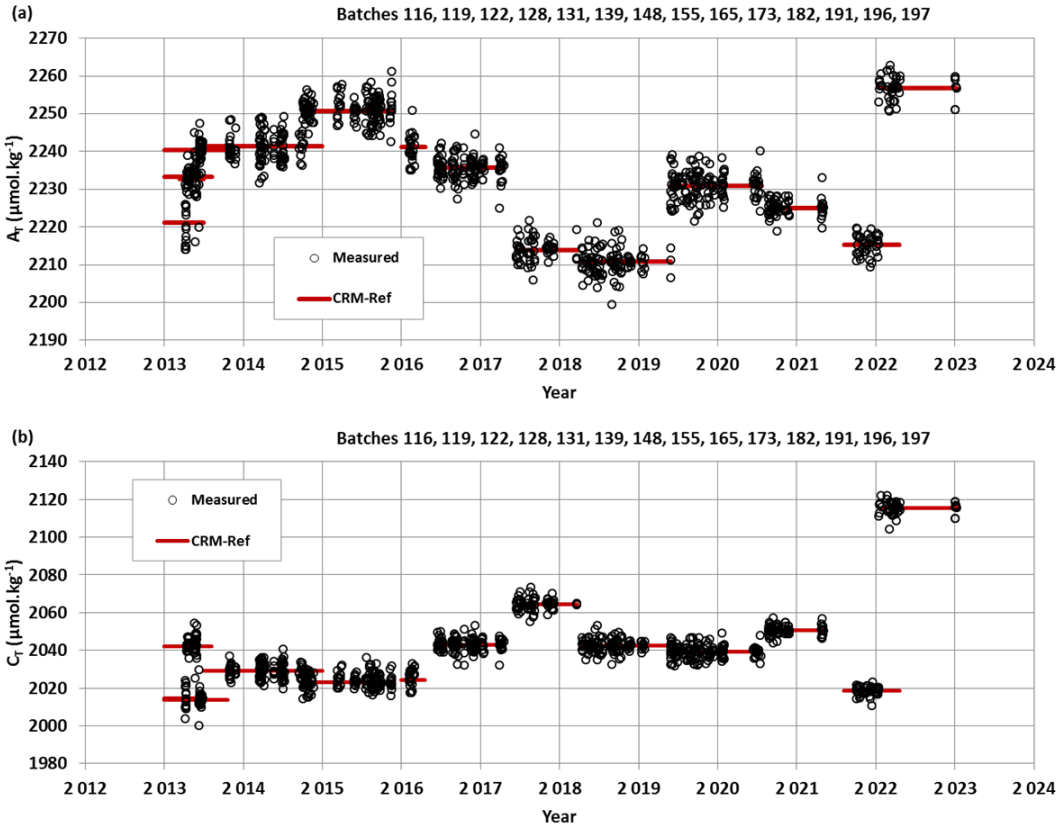

Figure 2: A_T (a) and C_T (b) analyses for different CRM Batches measured in 2013-2023. For these 965 analyses the mean and standard-deviations of the differences with the CRM reference were -0.1 (± 3.4) µmol kg^{-1} for A_T and 0.1 (± 3.7) µmol kg^{-1} for C_T.

3.2 Repeatability

For some projects, duplicates have been regularly sampled (SOMLIT-Point-B, SOMLIT-BREST, BOUSSOLE/DYFAMED) or replicate bottles sampled at selected depths at fixed stations during the cruises (e.g. OUTPACE-2015, SOMBA-2014). Results of A_T and C_T repeatability are synthetized in Table 2 and Figure 3 shows example of regular duplicates from the times-series SOMLIT-Point-B in the coastal Mediterranean Sea, SOMLIT-Brest in the Bay of Brest, coastal Iroise Sea and BOUSSOLE/DYFAMED in the Ligurian Sea. For the 26 OISO cruises conducted between 1998 and 2018 and the CLIM-EPARSES cruise in April 2019, the repeatability was evaluated from duplicate analyses (within 20 minutes time) of continuous sea surface underway sampling at the same location (when the ship was stopped). Similarly to what was found for the CRM measurements (Figure S2), differences in duplicates are occasionally higher than 10-15 µmol kg^{-1} (Figure 3) but most of the duplicates for all projects are within 0 to 3 µmol kg^{-1}. Based on the CRM analyses and replicates for

different projects, different regions and different periods, we estimated A_T and C_T data to be consistent to better than 4 µmol kg^{-1}.

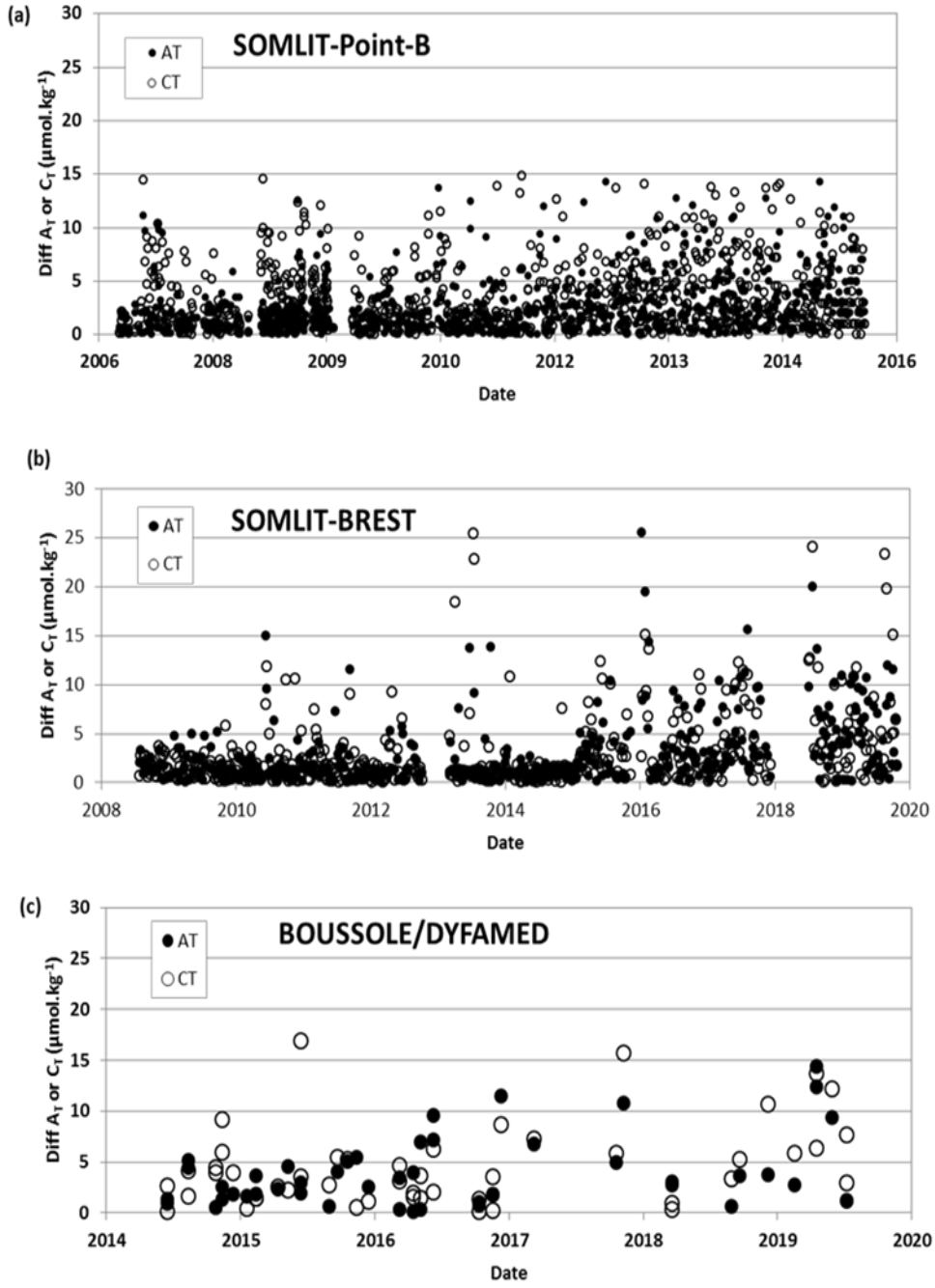

Figure 3: Results of duplicate A_T and C_T analyses from the time-series (a) SOMLIT-Point-B in the coastal Mediterranean Sea (Kapsenberg et al., 2017), (b) SOMLIT-BREST in the Bay of Brest, coastal Iroise Sea (Salt et al., 2016 and unpublished) and (c) BOUSSOLE/DYFAMED in the Ligurian Sea (Merlivat et al., 2018; Golbol et al., 2020). The plots show differences in duplicates for both A_T (filled circles) and C_T (open circles). Standard-deviations of these duplicates are listed in Table 2.

Table 2: Repeatability of A_T and C_T analyses for cruises with duplicate analysis. The results are expressed as the standard-deviations (Std) of the analysis of replicated samples. Nb = the number of replicates for each Time-series or Cruise (a). For the 26 OISO cruises (1998-2018) and for simplicity we list the mean repeatability obtained for all cruises.

Cruise	Nb	Std A_T µmol kg^{-1}	Std C_T µmol kg^{-1}	Reference
OUTPACE	12	3.64	3.68	Wagener et al. (2018)
SOMBA	13	2.00	3.30	Keraghel et al. (2020)
SOMLIT-Point-B	786	2.63	3.10	Kapsenberg et al. (2017)
SOMLIT-Brest	446	3.34	3.67	Salt et al. (2016) + unpub
BOUSSOLE	48	3.47	4.02	Merlivat et al. (2018); Golbol et al. (2020)
CLIM-EPARSES	122	2.20	2.30	Lo Monaco et al. (2020, 2021)
OISO 1998-2018	1162	2.06	2.28	Metzl et al. (2006) and (b)

(a) See Figure 3 for the results of regular duplicates for 3 time-series (SOMLIT-Point-B, SOMLIT-BREST, and BOUSSOLE).
(b) Metadata and data available at www.nodc.noaa.gov/ocads/oceans/VOS_Program/OISO.html

3.3 Inter-comparisons

Inter-comparisons of measurements performed with different technics help to evaluate the quality of the data and detect potential biases when merging the data in the same region obtained by different laboratories at different periods. This is especially important to interpret long-term trends of A_T and C_T as well as for pCO_2 and pH calculated with A_T/C_T pairs. For ocean acidification studies, this also refers to the "climate goal" for which an accuracy for A_T and C_T better than ±2 µmol kg^{-1} is needed (Newton et al., 2015; Tilbrook et al., 2019). For the projects in this data synthesis, inter-laboratory comparisons were performed occasionally and summarized below.

3.3.1 CHANNEL project

As part of the time-series CHANNEL (2012-2015) in the Western English Channel, Marrec et al. (2014) analyzed surface samples collected bi-monthly in 2011-2013. A_T analyses were performed with a TA-ALK-2 system (Appolo SciTech.) while C_T measurements were acquired with an AIRICA system (Marianda Inc.) Based on CRM analyses (Batch #92) the accuracy was estimated ±3 µmol kg^{-1} for A_T and ±1.5 µmol kg^{-1} for C_T (Marrec et al., 2014). When comparing with the samples measured at LOCEAN/Paris for the year 2012, Marrec et al. (2014) concluded that between the two methods the concentrations were within ±2 µmol kg^{-1} and ±3 µmol kg^{-1} for A_T and C_T respectively. This is close to the "climate goal" offering confident results for long-term trend analysis of the carbonate system in this region.

3.3.2 SURATLANT project

In the frame of the SURATLANT project in the subpolar North Atlantic gyre, some samples collected at the same time (in 2005, 2006, 2010, 2015, and 2016) were also analyzed onshore for A_T and/or C_T by other

laboratories using different technics (e.g. coulometric method) and the results summarized by Reverdin et al. (2018). For C_T, the mean (and STD) differences between LOCEAN values and from 4 other laboratories range between -0.7 (±4.6) and -6.5 (±3.4) μmol kg^{-1} depending on the cruise. For A_T the mean differences with 2 other laboratories range from -0.6 (±4.1) μmol kg^{-1} to +2.3 (±4.8) μmol kg^{-1}.

3.3.3 OVIDE project

During OVIDE cruises conducted since 2002 in the North Atlantic along a section from Greenland to Portugal (Lherminier et al., 2007; Mercier et al., 2015) samples have been taken (since 2006) to complement, for summer, the SURATLANT time-series in the North Atlantic subpolar gyre (NASPG). The OVIDE samples at the surface and along the water-column at a few stations were measured back at LOCEAN for A_T and C_T (Metzl et al., 2018). This enables us to compare our data with the measurements performed on-board by the IIM group in Vigo/Spain (e.g. Pérez et al., 2010, 2013, 2018; Vazquez-Rodriguez et al., 2012). The OVIDE data have been regularly quality controlled in CARINA and GLODAP data products (Velo et al., 2009; Key et al., 2010; Olsen et al., 2016, 2019, 2020). The results of inter-comparisons are gathered in Table 3. For OVIDE in 2006 we identified (for unknown reason) a large difference between our original A_T values compared to the A_T data qualified in GLODAP and we thus corrected our A_T data by +7.2 μmol kg^{-1}. However, no correction was applied for C_T. For other OVIDE cruises, differences for A_T range between -4.5 (±4.11) μmol kg^{-1} and -0.05 (±3.43) μmol kg^{-1} depending on the cruise (i.e. A_T measured at LOCEAN was always slightly lower than onboard measurements). For C_T, we compared our measurements onshore with C_T values calculated with A_T and pH measured onboard. Most of the mean C_T differences are slightly positive (i.e. C_T measured at LOCEAN was always higher, except for 2010). Taking into account all errors associated with the sampling, the transport of samples, the instrumentations, the data processing, or the calculations for C_T using A_T/pH pairs (around 8.8 μmol kg^{-1}, Orr et al, 2018), the comparisons between LOCEAN and IIM data for OVIDE cruises are deemed acceptable and large differences for both A_T and C_T (> 4 μmol kg^{-1}) are far from being systematic (Table 3). The data from SURATLANT and OVIDE can then be merged to complete the time-series in the NASPG in summer and to better describe the seasonality of the oceanic carbonate system. For example, in 2010, when the North Atlantic Oscillation (NAO) was strongly negative, the SURATLANT data showed a rapid decrease of C_T concentrations in the NASPG between early June and August (Figure 4), with C_T concentrations in August much lower than other years (Racapé et al., 2014). This leads to a rapid drop in fCO_2 in 2009-2010, such that the NASPG was a strong CO_2 sink (Leseurre et al., 2020). The winter-to-summer seasonal decrease of C_T in 2010 in the north NASPG was on average -77 μmol kg^{-1} (Figure 4) much larger than in the climatology (range -50 to -55 μmol kg^{-1}, Takahashi et al., 2014; Reverdin et al., 2018). The OVIDE data in late June 2010 and SURATLANT in August 2010 confirmed this signal that was linked to a pronounced primary productivity in that period (Figure 4, Henson et al., 2013; Racapé et al., 2014; Mc Kinley et al., 2018). Notice that for this period no fCO_2 observations were available in July-September 2010 in SOCAT data product and the A_T/C_T data presented here could be used to calculate fCO_2 to complement the fCO_2 dataset in this region like was done for other periods (Mc Kinley et al., 2011).

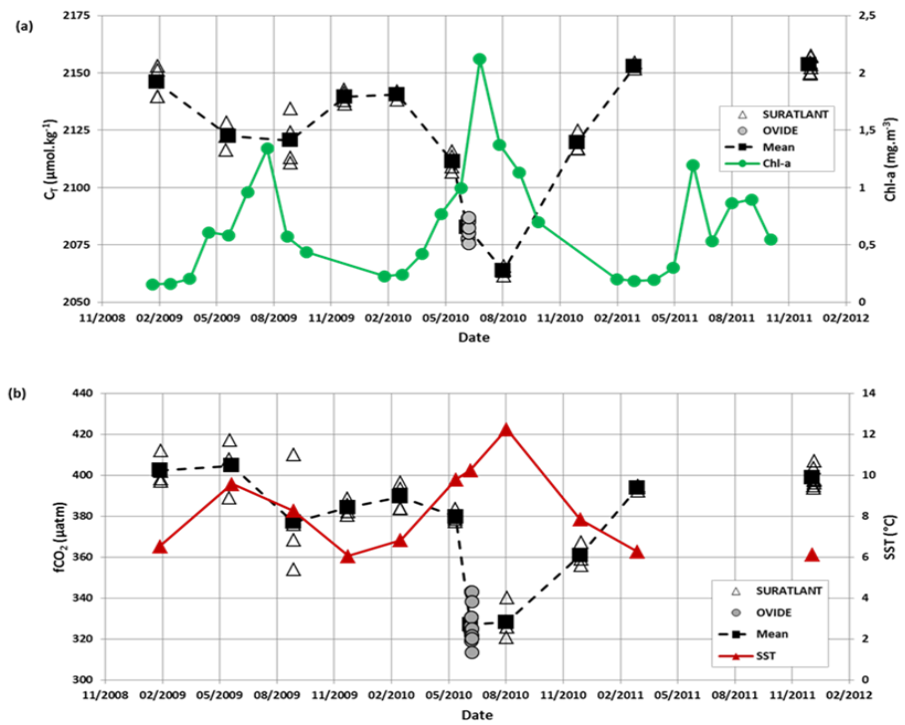

Figure 4: (a) Time-series of C_T concentrations (µmol.kg^{-1}) for 2009-2011 in surface waters in the North Atlantic subpolar gyre (zone 59°N-33°W) based on SURATLANT (open triangles) and OVIDE-2010 (grey circles) data. In 2009, SURATLANT data were available in February, June, September and December, while in 2010 data available in March, June, August and December and in 2011 data only available for March and December. The OVIDE data in late June 2010 completed the temporal cycle and confirmed the strong seasonal signal and low C_T concentrations in summer 2010 not seen in 2009 (or in 2011 as there is no data in summer). The mean observations for each period describe the C_T seasonal cycles in 2009 and 2010 (Black squares, dashed line). The monthly surface chlorophyll-a concentrations (Chl-a, mg.m^{-3}) averaged in the same region based on MODIS are also shown (Green dots and line) highlighting the high productivity during the summer 2010. Chl-a monthly data extracted from MODIS (Giovanni/NASA, last access 3/5/19). (b): Time-series of fCO_2 (µatm) for the same cruises (same symbols) calculated with A_T/C_T and using the K1, K2 constants from Lueker et al (2000). Mean SST (°C) indicated (red triangles). In June 2010 oceanic fCO_2 decreased by 53 µatm in 2 weeks.

Table 3: Comparisons of A_T and C_T samples measured back at LOCEAN with measurements onboard by IIM Laboratory (F. Pérez, Vigo, Spain) for OVIDE cruises in the North Atlantic. Nb= Number of samples. ND= No Data. The results listed indicate the mean and standard-deviations of the differences (LOCEAN-IIM). For A_T, IIM values were measured on-board. For C_T, IIM values were calculated from A_T and pH both measured onboard. The IIM data were quality controlled and here taken from the GLODAP data products (Olsen et al, 2016, 2019).

Cruise Year	Nb A_T	A_T (LOCEAN) – A_T (IIM) µmol kg^{-1}	Nb C_T	C_T (LOCEAN) – C_T (IIM) µmol kg^{-1}
OVIDE-2006	14	-2.0 (± 5.9) (*)	14	1.1 (±2.5)
OVIDE-2008	29	-4.5 (± 4.1)	29	3.8 (±3.1)
OVIDE-2010	41	-2.0 (± 2.3)	41	-2.4 (±3.3)
OVIDE-2012	37	-0.1 (± 8.8)	ND	ND
GEOVIDE-2014	57	-0.1 (± 3.4)	54	2.4 (±7.9)

(*) for the OVIDE 2006 cruise original difference for A_T was -9.0 (± 5.8) µmol kg^{-1} and LOCEAN A_T data were corrected by +7.2 µmol kg^{-1} based on the mean concentrations in deep layers. No corrections were applied for A_T and C_T for other cruises.

3.3.4 PENZE river

The comparisons described above concern the open ocean region with A_T and C_T concentrations in a range of concentrations close to the CRM references (used by the different laboratories). Another example of comparison is presented here for samples obtained along a river and thus for waters with low salinity and A_T concentrations (river Penzé in North Brittany). In 2019-2020, A_T was measured at SBR laboratory (Station Biologique de Roscoff) by a potentiometric method (using a Titrino-847 plus Metrohm) calibrated with CRM (Batch #131) for a final accuracy of ±2.1 µmol kg^{-1} (Gac et al., 2020). Although the samples were measured with different technics the A_T/Salinity relationships are very coherent for both datasets (Figure 5). The regressions for each period are for A_T (in µmol kg^{-1}):

In 2011 (78 samples): $A_T = 51.525\ (\pm 0.944)\ S + 583.95\ (\pm 19.94)$ ($r^2 = 0.975$)

In 2019-2020 (70 samples): $A_T = 54.022\ (\pm 1.018)\ S + 450.23\ (\pm 31.53)$ ($r^2 = 0.976$)

Therefore we added the A_T data measured in 2019-2020 to complete the synthesis for this location (river Penzé).

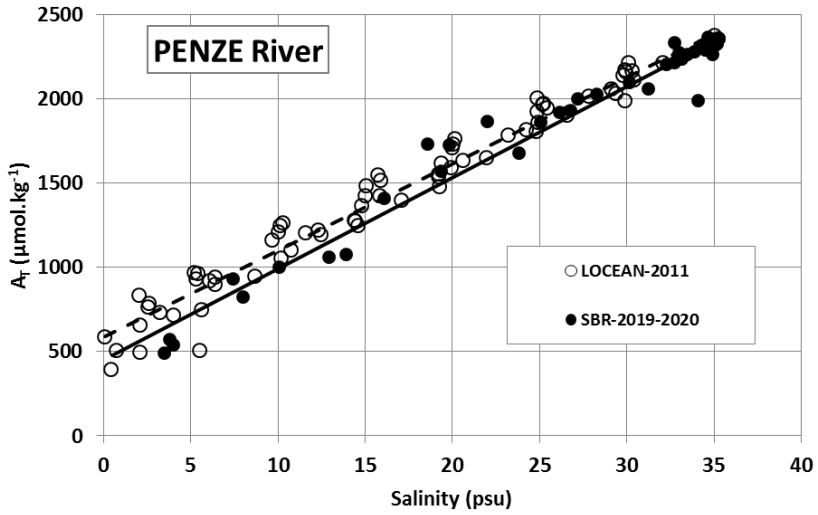

Figure 5: Total alkalinity (A_T) versus salinity for samples measured in 2011 and 2019 in the river Penzé, North Brittany (Gac et al., 2020). A_T samples were measured at LOCEAN in 2011 (open circles, dashed-line) and at SBR laboratory (Roscoff) in 2019 (filled circles, black line).

3.4 Quality control assigned flags

Identifying each data with an appropriate flag is very convenient for selecting the data (good, questionable or bad). Here we used 4 flags for each property (flags 2 = good, 3= questionable, 4=bad, and 9= no data) following the WOCE program and used in other data products such as SOCAT (Bakker et al., 2016) or GLODAP (Olsen et al., 2016, 2019, 2020; Lauvset et al., 2021). During the data-processing, we first assigned a flag for each A_T and C_T data based on the standard error in the calculation of A_T and C_T concentrations (non-linear regression, Dickson et al. 2007). By default, if the standard-deviation on the regression is > 1 µmol kg^{-1}, we assigned a flag 3 (questionable) although the data could be acceptable and then used for interpretations. Flag 3 was also assigned when salinity was doubtful or when differences of duplicates were large (e.g. ±20 µmol kg^{-1}). Flags 4 (bad or certainly bad) were assigned when clear anomalies were detected for unknown reason (e.g. a

sample probably not fixed with $HgCl_2$). A secondary quality control was performed by the PIs of each project based on data inspection, duplicates, A_T/Salinity relationship, or the mean observations in deep layers where large variability in A_T and C_T is unlikely to occur from year to year. An example presents all data from the MOOSE-GE cruises conducted in 2010-2019 in the Mediterranean Sea (Coppola et al., 2020; Testor et al., 2010) where clear outliers have been identified (Figure S3). For the 10 MOOSE-GE cruises and a total of 1847 A_T and C_T analyses, 26 were identified flagged as bad (flag 4), 139 for A_T and 141 for C_T listed as questionable (flag 3) and 1682 for A_T and 1680 for C_T considered as good data (flag 2, i.e. more than 90%). Similar control was performed for each project.

The synthesis of various cruises in the same region and period also offers verification and secondary control of the data. For example, several cruises were conducted in the Mediterranean Sea in 2014 (MOOSE-GE, SOMBA, ANTARES and DYFAMED). The mean values of C_T and A_T in the deep layers (> 1800m) for each cruise confirmed the coherence of the data (Table 4). This enabled to merge the different datasets for interpretations of the temporal trends and processes driving the CO_2 cycle (Coppola et al., 2019, 2020) or to train and validate a regional neural network to reconstruct the carbonate system (e.g. CANYON-MED, Fourrier et al., 2020, 2022).

Table 4: Mean observations in the deep layers (> 1800m) of the Western Mediterranean Sea for different cruises conducted in 2014. Results in deep layers (> 1800m) for the DEWEX cruise in 2013 and the PEACETIME cruise in 2017 in the same region are also listed. N-A_T and N-C_T are A_T and C_T normalized at salinity = 38. Nb = number of data (with flag 2). Standard-deviations are in brackets. References for these cruises are listed in Supplementary Material.

Cruise	Period	Nb	Pot. Temp (°C)	Salinity (PSU)	N-A_T (µmol kg^{-1})	N-C_T (µmol kg^{-1})
All cruises	Feb/Dec-2014	76	12.905 (0.007)	38.486 (0.005)	2562.9 (5.3)	2303.7 (4.7)
ANTARES	Feb/Nov-2014	14	12.913 (0.004)	38.488 (0.006)	2564.0 (3.8)	2301.9 (3.5)
DYFAMED	Mar/Dec-2014	9	12.905 (0.0016)	38.487 (0.004)	2560.1 (5.0)	2304.3 (6.8)
MOOSE-GE	Jul-2014	21	12.909 (0.004)	38.487 (0.005)	2565.6 (4.6)	2303.5 (4.1)
SOMBA	Aug/Sep-2014	32	12.899 (0.005)	38.483 (0.005)	2561.5 (5.6)	2304.6 (4.8)
DEWEX	Feb/Apr-2013	44	12.903 (0.010)	38.588 (0.006)	2556.0 (4.3)	2294.0 (5.7)
PEACETIME	May/Jun-2017	7	12.904 (0.002)	38.486 (0.003)	2567.2 (10.6)	2308.1 (8.9)

The total number of data for the Global Ocean and the Mediterranean Sea are gathered in Table 5 with corresponding flags for each property. Overall, the synthesis includes more than 94% of good data for both A_T

and C_T. About 5% are questionable and 2% are likely bad. Overall, we believe that all data (with flag 2) in this synthesis have an accuracy better than 4 µmol kg^{-1} for both A_T and C_T, the same as for quality-controlled data in GLODAP (Olsen et al., 2020; Lauvset et al., 2021). The uncertainty ranges between the "Climate goal" (2 µmol kg^{-1}) and the "Weather Goal" (10 µmol kg^{-1}) for ocean acidification studies (Newton et al., 2015; Tilbrook et al., 2019). This accuracy is also relevant to validate or constraint data-based methods that reconstruct A_T and C_T fields with an error of around 10-15 µmol kg^{-1} for both properties (Bittig et al., 2018; Broullón et al., 2019, 2020; Fourrier et al., 2020).

Table 5: Number of Temperature, Salinity, A_T and C_T data in the synthesis identified for flags 2, 3, 4, 9. The data are given for the full data-set Global Ocean and for the Mediterranean Sea. Last column is the percentage of flag 2 (Good).

	Flag 2	Flag 3	Flag 4	Flag 9	% Flag 2
Global Ocean					
Temperature	43538	410	0	478	99.07
Salinity	44033	319	2	71	99.28
A_T	39331	2144	1165	1787	92.24
C_T	39921	2091	1148	1279	92.50
Mediterranean Sea					
Temperature	9843	1	0	65	99.99
Salinity	9879	8	2	20	99.99
A_T	8853	425	411	220	91.37
C_T	8854	451	389	211	91.33

3.5 Using A_T and C_T to calculate fCO_2 and pH and compare with fCO_2 and pH measurements

For some projects, the A_T and C_T data presented in this synthesis were used to calibrate or validate in situ fCO_2 sensors (Bozec et al., 2011; Marrec et al., 2014; Merlivat et al., 2018). The A_T and C_T data were also used to calculate fCO_2 and to derive associated air-sea CO_2 fluxes, especially during periods when no direct fCO_2 measurements were available (e.g. in the North Atlantic, Figure 4, Watson et al., 2009; Mc Kinley et al., 2011). For example, Marrec et al. (2014) successfully used the calculated pCO_2 (with A_T/C_T pairs) to adjust the drift of the pCO_2 data recorded with a Contros-HydroC/CO2 FT sensor mounted on a FerryBox for regularly sampling the Western English Channel (CHANNEL project). Here we show the results for the period 2012-2014 (Figure 6). In this region the total alkalinity is relatively constant over time; the average of A_T for 528 samples at different seasons and years is 2334.4 (±7.2) µmol kg^{-1}. On the opposite, the C_T concentrations show distinctive seasonality, with higher concentrations in winter and lower in summer when biological activity is pronounced (Marrec et al., 2013, 2014; Kitidis et al., 2019). This controls the seasonal pCO_2 distribution revealed each year in both measured and calculated pCO_2 (Figure 6). For 528 co-located samples the mean difference between calculated and measured pCO_2 is -1.9 (±11.9) µatm with no distinct differences depending on the season and year.

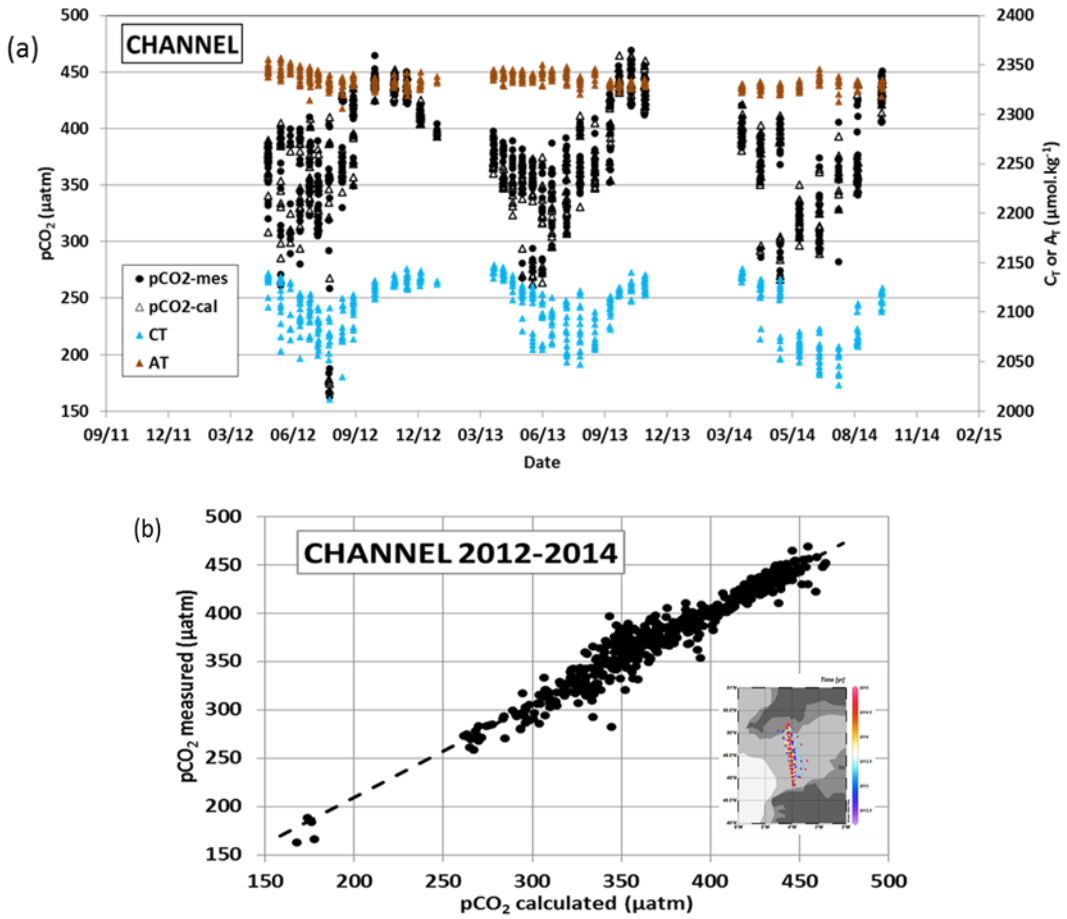

Figure 6: (a): Time-series of A_T (brown triangles, right Y-axis), C_T (blue triangles, right Y-axis), pCO_2 calculated (open triangles, left Y-axis) and pCO_2 measured (filled circles) in the Western English Channel in 2012-2014 (Marrec et al., 2014). (b): Measured pCO_2 versus calculated pCO_2 for the same samples. The mean difference (pCO_{2cal}-pCO_{2mes}) for 528 samples is -1.9 µatm (± 11.9) µatm. Data from Marrec and Bozec (2016 a,b; 2017). Localization of the samples is shown in the inserted map.

In the Ligurian Sea, following the first high frequency in situ fCO_2 measurements in 1995-1997 at the DYFAMED time-series station (Hood and Merlivat, 2001), a new CARIOCA fCO_2 sensor was deployed at that location in 2013 (BOUSSOLE project, Merlivat et al., 2018). The CARIOCA sensor was calibrated with regular A_T/C_T analyses performed at LOCEAN. Based on these data, the mean difference between CARIOCA-fCO_2 measurements and calculated-fCO_2 data was estimated to be around ±4.4 µatm for 2013-2015, i.e. the same order than the precision of the CARIOCA sensor (±5 µatm, Merlivat et al., 2018). Here we extend the results for the period 2013-2018 (Golbol et al., 2020; data also in SOCAT version v2021, Bakker et al., 2016) and compared the CARIOCA fCO_2 time-series with A_T and C_T data from different cruises (BOUSSOLE, DYFAMED and MOOSE-GE) selected in the layer 0-20m at that location (Figure S4). For 67 co-located samples at different seasons and years, the mean difference between calculated and measured fCO_2 (fCO_{2cal}-fCO_{2mes}) was -3.7 µatm (± 10.8) µatm where fCO_2 was calculated from A_T/C_T pairs using the constant from Lueker et al (2000). At that location, the alkalinity is relatively constant over 2013-2018 with an average concentration of 2569.8 (±13.2) µmol kg^{-1}. C_T concentrations show a clear seasonality, decreasing by around 50 µmol kg^{-1} from winter to late summer driving the large seasonal cycle of fCO_2 (range 80 µatm) revealed in both measured and calculated values (here fCO_2 is normalized at 13°C, Figure S4). In addition to calibration purposes, a regional A_T/Salinity relationship was derived from the A_T data measured at that location and successfully used to construct time-

series of C_T and pH calculated from the high-frequency CARIOCA fCO_2 data to investigate and interpret the long-term change of fCO_2 and acidification in the Ligurian Sea (Merlivat et al., 2018; Coppola et al., 2020).

A CARIOCA sensor was also deployed in 2003 near the SOMLIT-Brest time-series site in the Bay of Brest (Bozec et al., 2011; Salt et al., 2016). As for BOUSSOLE in the Ligurian Sea, samples collected for A_T and C_T were used for validation of the pCO_2 recorded by the CARIOCA sensor and the comparison with calculated pCO_2 showed a good agreement, i.e. $pCO_{2cal} = 0.98* pCO_{2mes} + 7$ µatm (Bozec et al., 2011). CARIOCA sensors were also deployed on moorings in the Tropical Atlantic (PIRATA project, e.g. Lefèvre et al., 2008, 2016; Parard et al., 2010). With the discrete A_T and C_T data included in this synthesis (EGEE and PIRATA-FR cruises), the fCO_2 data from CARIOCA sensor associated with an adapted A_T/Salinity relationship were used to derive pH (Lefèvre et al., 2016) or C_T time-series to evaluate net community production in the Eastern tropical Atlantic (Parard et al., 2010; Lefèvre and Merlivat 2012).

Although this is not a direct instrumental inter-comparison, differences between pCO_2 (or fCO_2) calculated using A_T/C_T pairs with direct pCO_2 measurements give a glimpse of the quality of A_T and C_T data in this synthesis given the uncertainty attached to the pCO_2 or pH calculations (Orr et al., 2015). For example, in the frame of the SURATLANT project in the North Atlantic, calculated fCO_2 data were compared with co-located fCO_2 measurements for different seasons and years (Figure S5). The mean differences (fCO_{2cal}- fCO_{2mes}) ranged between -4.3 µatm (± 12.9) µatm (2004-2007, 74 co-located samples) and -3.0 (±12.1) µatm (2014-2015, 98 co-located samples). The differences are almost the same for different years (and seasons) and are thus attributed to method uncertainties (including sampling time, measurement errors, and data processing). Based on these comparisons and the consistency between data we are confident that the A_T and C_T data presented in this synthesis could be used to calculate fCO_2 (and pH) and interpret temporal changes and drivers of these parameters as well as to estimate air-sea CO_2 fluxes in the North Atlantic (e.g. Corbière et al., 2007; Schuster et al., 2009, 2013; Watson et al., 2009; Metzl et al., 2010; Mc Kinley et al., 2011; Reverdin et al., 2018, Kitidis et al., 2019; Leseurre et al., 2020).

The A_T and C_T data in this synthesis have been also successfully used for fCO_2 and air-sea CO_2 fluxes calculations in other regions: the tropical Atlantic (Koffi et al., 2010), the tropical Pacific (Moutin et al., 2018; Wagener et al., 2018), the Solomon sea (Ganachaud et al., 2017) or the Mediterranean sea and coastal zones (De Carlo et al., 2013; Marrec et al., 2015; Kapsenberg et al., 2017; Coppola et al., 2020; Keraghel et al., 2020; Wimart-Rousseau et al., 2020a; Gattuso et al., 2023).

In addition, A_T and C_T data in the surface and the water-column are also relevant to calculate pH and evaluate its rate of change for addressing ocean acidification topic in different regions (Kapsenberg et al., 2017; Ganachaud et al., 2017; Wagener et al., 2018; Coppola et al., 2020; Leseurre et al., 2020; Lo Monaco et al., 2021). At the time-series station ECOSCOPA in the Bay of Brest (Fleury et al., 2023; Petton et al., 2023), pH calculated with A_T/C_T data were compared with direct pH measurements (Figure S6). In 2017-2019, pH (at standard temperature 25°C, pH-25C) was always lower than 8 and presented a large seasonal signal of 0.3 (high pH values in spring, low in winter). The mean difference between calculated and measured pH-25C for 46 samples was equal to +0.013 (± 0.010) which is in the range of the pH uncertainty evaluated by error propagation when calculated from A_T/C_T pairs (A_T and C_T error of ±3 µmol kg^{-1} leads to pH error of ±0.0144). Part of these A_T and C_T data used to calculate pH also helped for interpreting the response of marine species to acidification, e.g. pteropodes or coccolithophores (*Emiliana huxleyi)* in the Mediterranean Sea (Howes et al., 2015, 2017; Meier et al., 2014) or in the Southern Ocean (Beaufort et al., 2011). The A_T and C_T data were also

supporting environmental analysis in coral reef ecosystems in the tropical Pacific (TARA Expedition, Douville et al., 2022; Lombard et al., 2023; Canesi et al., 2023).

4 Global distribution and relationships from A_T and C_T based on the SNAPO-CO2 dataset

The surface distribution in the global ocean based on the SNAPO-CO2 dataset is presented in Figure 7 for A_T and C_T. In the open ocean, high A_T concentrations are identified in the subtropics in all basins (Jiang et al., 2014; Takahashi et al., 2014) with highest concentrations up to 2484 µmol kg^{-1} in the central North Atlantic (STRASSE cruise in August 2012, 26°N/36°W). In surface and at depth, the A_T/Salinity and A_T/C_T relationships are clearly identified and structured at regional scale (Figure 8).

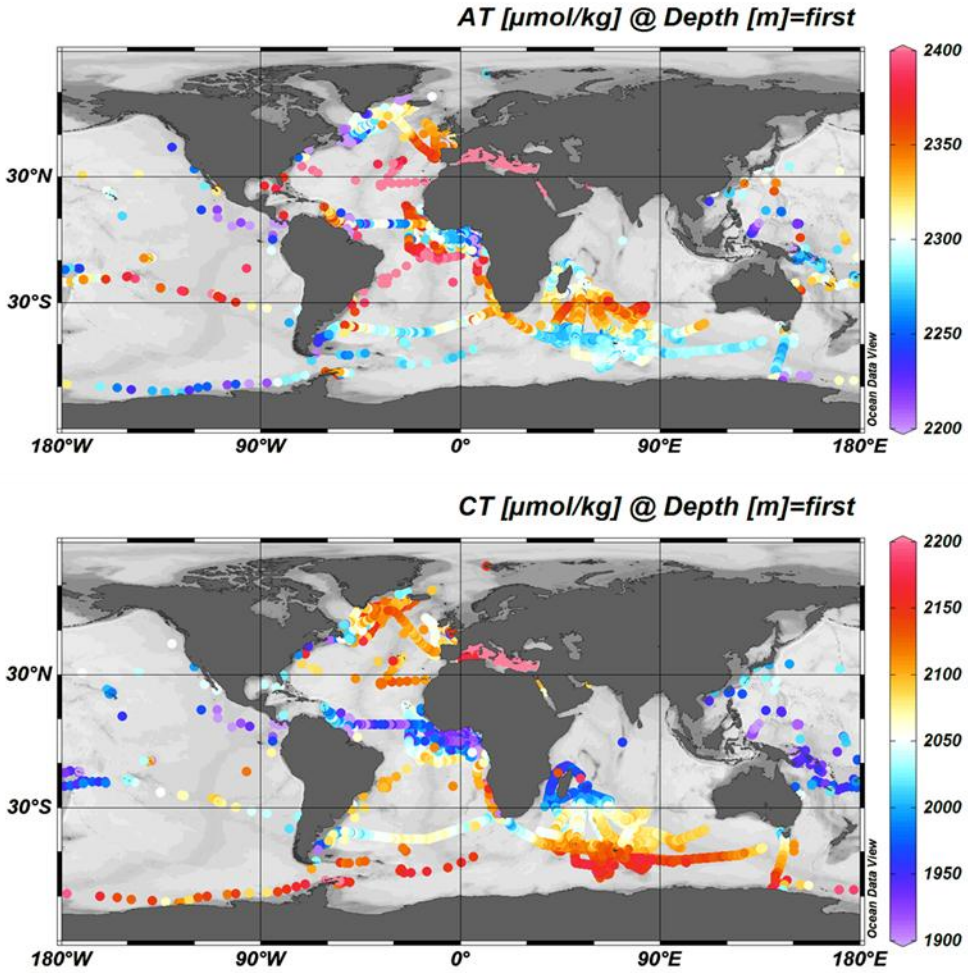

Figure 7: Distribution of A_T (top) and C_T (bottom) concentrations (µmol.kg^{-1}) in surface waters (0-10m). Only data with flag 2 are presented in these figures. Figures produced with ODV (Schlitzer, 2018).

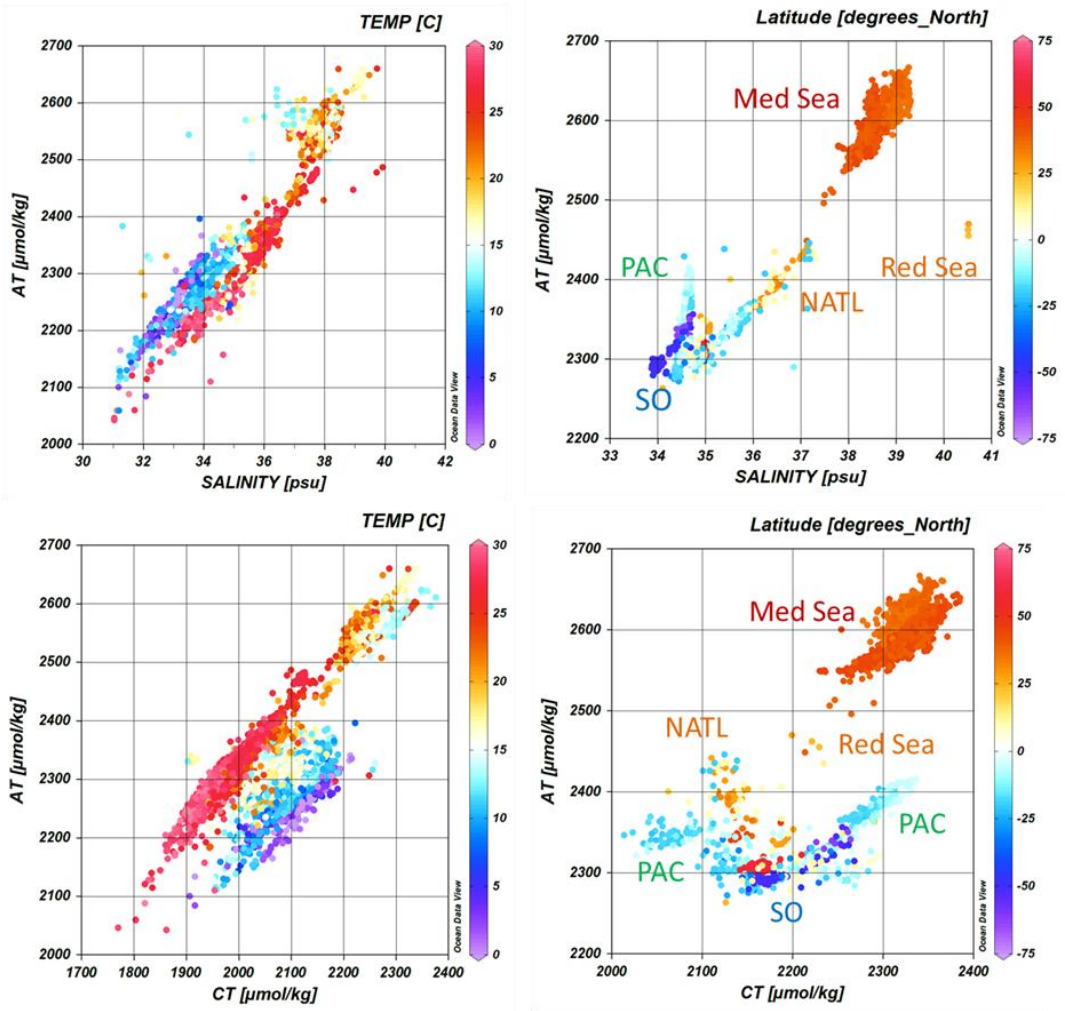

Figure 8: Relationships between A_T and Salinity (upper panel) and A_T versus C_T (lower panel) for samples in surface waters (0-10m and SSS > 31) (left) and in the water column below 100m (right). Only data with flag 2 are presented. The color scales correspond to the temperature (left) or the latitude (right). Some location of data are identified: Mediterranean Sea (Med Sea), Red Sea, Tropical Pacific (PAC), North Atlantic (NATL) and Southern Ocean (SO). Figures produced with ODV (Schlitzer, 2018).

In the Eastern tropical Atlantic (ETA) where the Congo River impacts the salinity field (Vangriesheim et al., 2009), A_T concentrations range between 2100 and 2400 µmol kg^{-1}. The regional A_T/Salinity relationship in the ETA based on data from the EGEE cruises in 2005-2007 (Koffi et al., 2010) is robust and validated with more recent measurements from PIRATA-FR cruises in 2010-2019 (Lefevre et al., 2021). The strong A_T/Salinity relationship in the ETA was also recognized using data from the TARA-MICROBIOME cruise in May-July 2022 (Figure S7). Low salinity (< 30) and low A_T (1700-2200 µmol kg^{-1}) are also observed in the Western tropical Atlantic near the Amazon River plume. The A_T/Salinity relationships in both river plume regions are very similar (Figure S7).

For C_T, the lowest concentrations were observed in the coastal regions of the Tropical Atlantic, on the eastern side in the Gulf of Guinea (BIOZAIRE cruise in 2003, 6°S/11°E, C_T=1390 µmol kg^{-1}, Vangriesheim et al., 2009) and on the Western side in coastal zone off French Guyana (PLUMAND cruise in 2007, 5°N/51°W, C_T=1512 µmol kg^{-1}, Lefèvre et al., 2010). Such low C_T concentrations were also observed around 5°N/51°W in the Amazon River plume during the recent EUREC4A-OA cruise in 2020 and the TARA-MICROBIOME cruise in 2021 (C_T=1451 µmol kg^{-1}) leading to low oceanic fCO_2 (< 350 µatm) and a CO_2 sink in this region (Olivier et al., 2022).

The high C_T concentrations were mainly observed in the Southern Ocean (OISO and ACE cruises) south of the Polar Front around 50°S linked to the upwelling of C_T-rich deep water (Figure 7, Metzl et al., 2006; Wu et al., 2019; Chen et al., 2022). This leads to a high C_T/A_T ratio and a high Revelle factor in the Southern Ocean (Figure 9, Fassbender et al., 2017). The high C_T content and low temperature in the Southern Ocean also lead to low calcite and aragonite saturation state (Ω) (Takahashi et al., 2014; Jiang et al., 2015). We calculate Ω from A_T and C_T data at insitu temperature, salinity and pressure. At present the surface ocean is not under-saturated with regard to aragonite (Figure 10); however, under-saturation levels (Ω-Ar<1) were found around 500 m in the Southern Ocean (ACE cruise in 2017, MODYDICK cruise in 2018), 1000 m in the Tropical Pacific (PANDORA 2012 and OUTPACE 2015 cruises) and 2200 m in the North Atlantic (OVIDE 2012 and 2014 cruises, see also Turk et al., 2017) (Figure 10). Samples at 400 m from the TARA-Oceans cruise in 2009-2012 also indicated aragonite under-saturation in the Equatorial Atlantic, Equatorial Pacific, as well as off South America (73°W-34°S, Chile) associated to equatorial or eastern boundary upwelling systems (Feely et al., 2012; Lauvset et al., 2020).

In surface, Ω–Ar>3 is found in the latitudinal band 45°S-54°N and Ω–Ar<3, below the critical threshold of Ω–Ar=3.25 that represents a limit for distribution of tropical coral reefs (Hoegh-Guldberg et al., 2007) is observed at very few locations in the tropics.

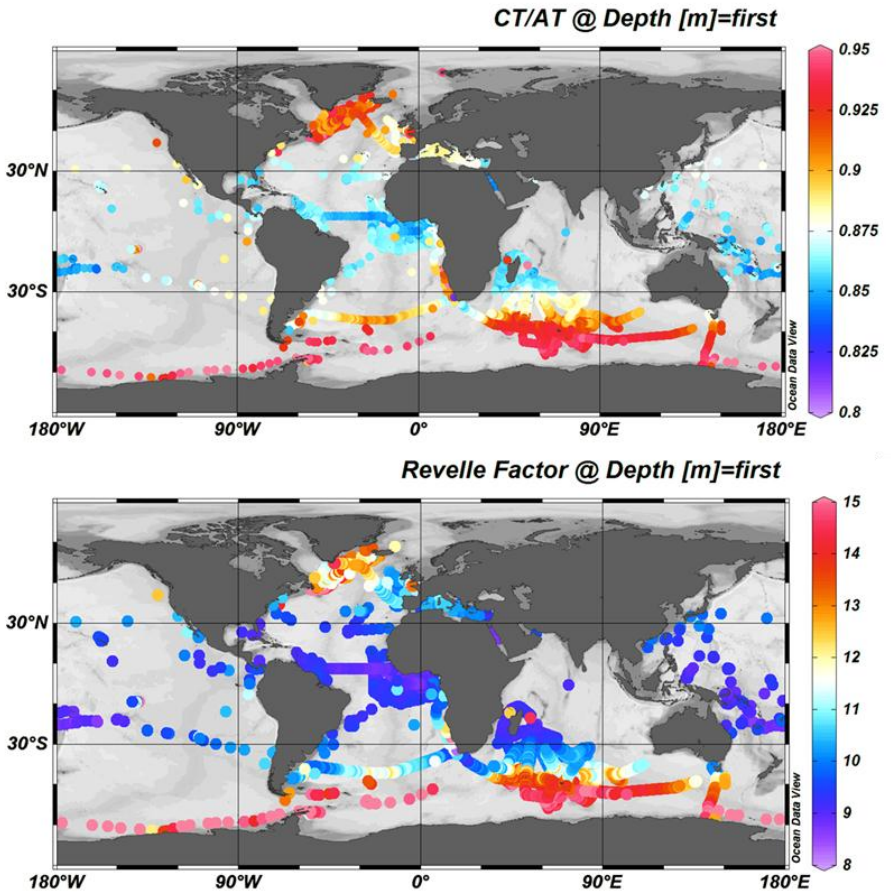

Figure 9: Distribution of the C_T/A_T ratio (top) and the Revelle factor (bottom) in surface waters (0-10m). Only data with flag 2 were used. Figures produced with ODV (Schlitzer, 2018).

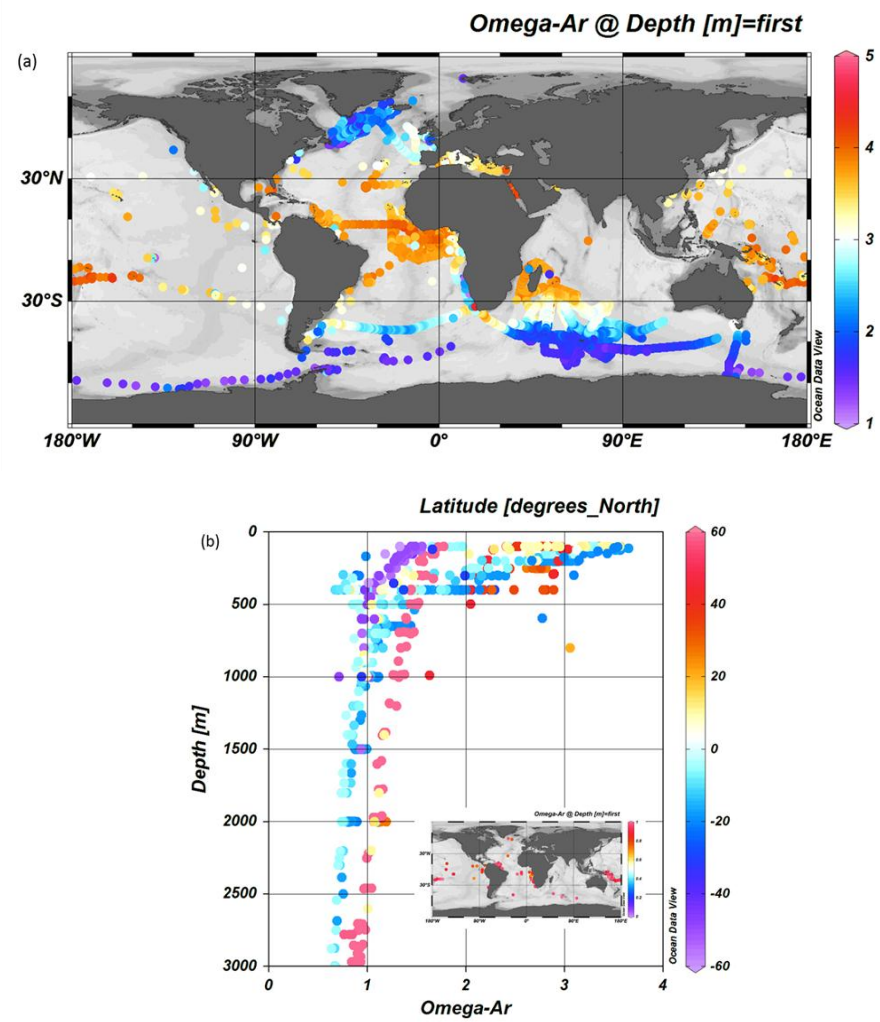

Figure 10: (a): Distribution of the aragonite saturation state (Ω-Ar) in surface waters (0-10m). Only data with flag 2 were used. (b): Depth profiles (100-3000m) of Ω-Ar at few locations in the Tropical Pacific, Atlantic and Southern Oceans. Stations where under-saturation is detected (Ω-Ar<1) at depth are identified in the inserted map. Figures produced with ODV (Schlitzer, 2018).

Compared to the open ocean, A_T concentrations are much higher in the Mediterranean Sea (Copin-Montégut, 1993; Schneider et al., 2007; Álvarez et al., 2023) with values up to 2600 µmol kg^{-1} (Figure 8). The A_T and C_T data obtained in 1998-2019 show on average a clear contrast between the northern and southern regions of the Western Mediterranean sea (Figure 11 a, b) with higher concentration in the Ligurian Sea and the Gulf of Lion (Gemayel et al., 2015). However, the basin scale average distribution view smoothed the meso-scale signals recognized in the Mediterranean Sea (e.g. Bosse et al., 2017; Petrenko et al., 2017). In the Gulf of Lion the synthesis of 11 cruises conducted from May 2010 to June 2011 (CARBORHONE, CASCADE, LATEX, MOLA, MOOSE-GE) highlights the contrasting distributions of A_T and C_T in the coastal zones and off shore (Figure 11 c, d). The averaging of all data in 1998-2019 also smoothed the seasonal signal and the inter-annual variability described below.

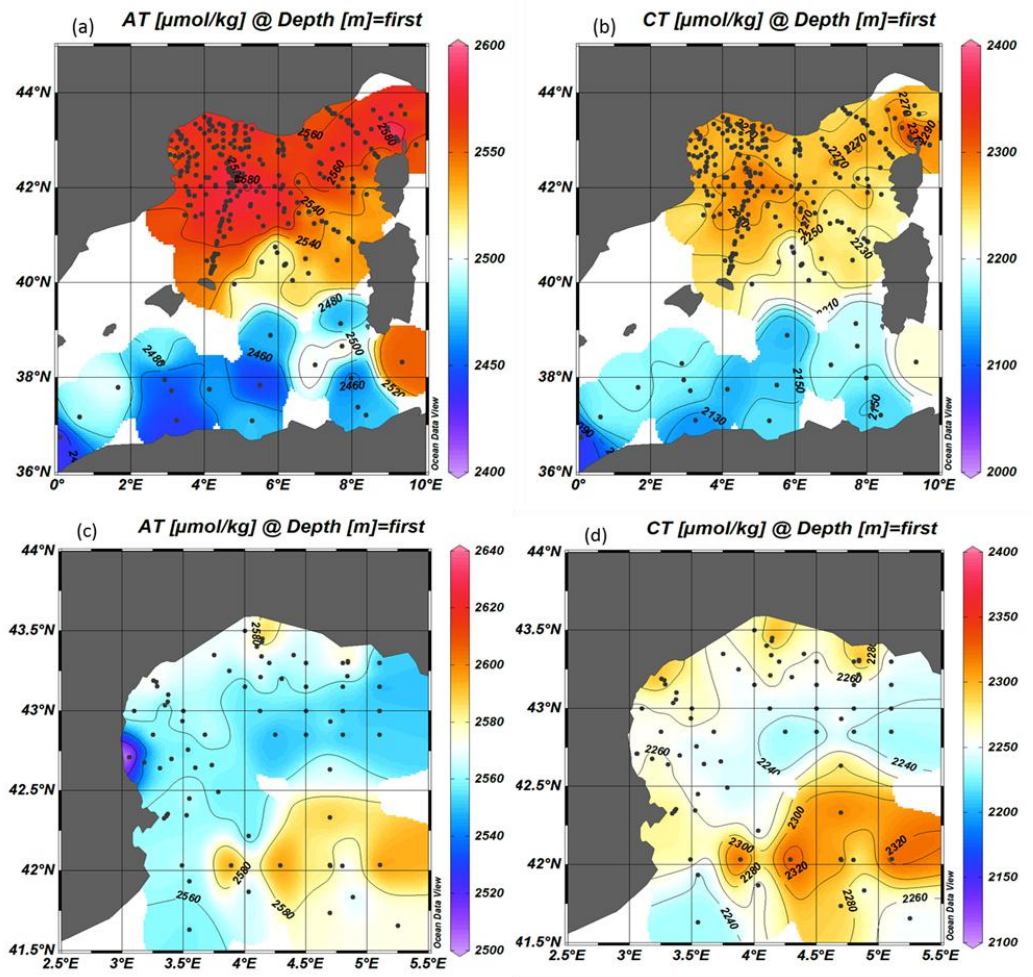

Figure 11: Distribution of A_T (a) and C_T (b) in µmol kg^{-1} in surface waters of the Western Mediterranean Sea (0-10m) from all data for 1998-2019. Detailed distribution of A_T (c) and C_T (d) in µmol kg^{-1} in surface waters of the Gulf of Lion for the period 2010-2011 only (cruises CARBORHONE, CASCADE, LATEX, MOLA, MOOSE-GE). Figures produced with ODV (Schlitzer, 2018).

5 Temporal variations of A_T and C_T: examples from the SNAPO-CO2 dataset

Time-series stations such as BATS, ESTOC, HOT in the subtropics and stations in the Irminger Sea or in the Iceland Sea are the only way to detect the long-term change in the ocean carbonate system in the surface and the water column (Bates et al., 2014). These important time-series help to understand driving processes (e.g. Hagens and Middelburg, 2016) and are often used to validate the pCO_2, A_T, C_T, or pH reconstructed fields (e.g. Rödenbeck et al., 2013; Broullón et al., 2019, 2020; Keppler et al., 2020; Gregor and Gruber, 2021; Chau et al., 2023; Ma et al., 2023).

Here we show examples of the temporal surface variations at locations where data were obtained for more than 10 years (Figure 12). We thus selected the following contrasting regions: the North Atlantic subpolar gyre (NASPG around 60°N/30°W, period 1993-2018), the Equatorial Atlantic (at 2°N-2°S/12°W-8°W, period 2005-2017), the Indian Ocean subtropical sector (26-35°S/50-56°E, period 1998-2018), the Indian Ocean high latitude (54-60°S/60-70°E, period 1998-2018), the Ligurian Sea (around DYFAMED station, 43.5-42.5°N/5.5-9°E, period 1998-2019) and times-series stations in the coastal zones off Britanny (period 2008-2019).

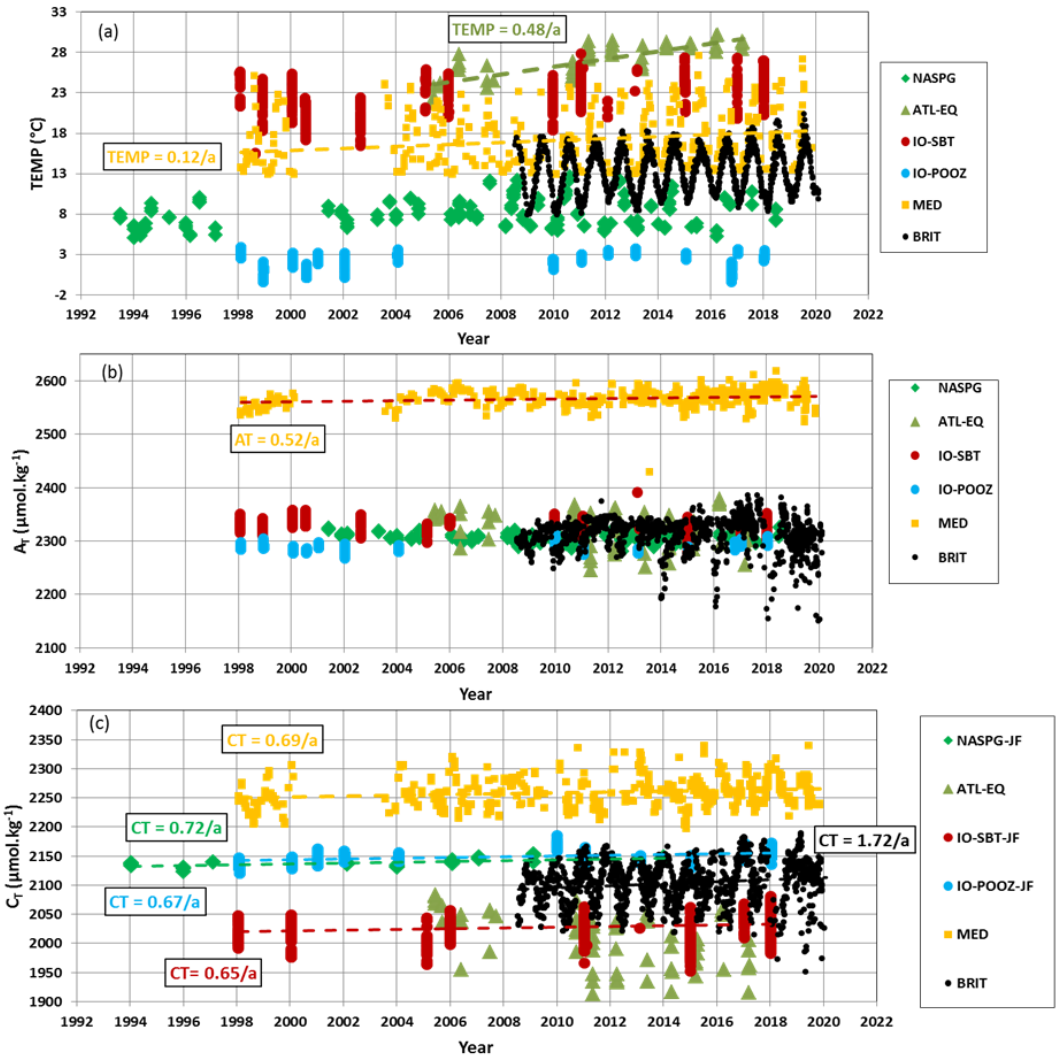

Figure 12: Time-series of (a) sea surface temperature (°C), (b) A_T (µmol kg^{-1}) and (c) C_T (µmol kg^{-1}) in 6 regions: the North Atlantic subpolar gyre (NASPG 1993-2018, green diamond), the Equatorial Atlantic (ATL-EQ, 2005-2017, green triangle), the Indian subtropical sector (IO-SBT, red circle) and high latitude (IO-POOZ, blue circle) (1998-2018), the Ligurian Sea (MED, 1998-2019, orange square) and times-series stations in the coastal zones off Brittany (BRIT, period 2008-2019, black dots). Trends (dashed lines and values) are shown when relevant for the discussion (C_T trends listed in Table 6).

Table 6: Trend of C_T (µmol kg^{-1} yr^{-1}) and corresponding standard error in 5 selected regions where data were available for more than 10 years (data are shown in Figure 12). The projects/cruises for selection of the data in each domain are indicated.

Region (acronym)	Period	C_T trend (µmol kg^{-1} yr^{-1})	Season	Projects/Cruises
North Atlantic (NASPG)	1994-2014	+0.72 (0.17)	Jan-Feb	SURATLANT
Indian Subtropic (IO-SBT)	1998-2018	+0.65 (0.12)	Jan-Feb	OISO
Indian South. (IO-POOZ)	1998-2018	+0.67 (0.04)	Jan-Feb	OISO
Ligurian Sea (MED)	1998-2019	+0.68 (0.18)	All seasons	DYFAMED, BOUSSOLE, MOOSE-GE
Coast Brittany (BRIT)	2008-2019	+1.72 (0.28)	All seasons	Brest, Roscoff, ECOSCOPA, PENZE

In the 6 regions, there was a progressive warming most clearly detected in the Mediterranean Sea (e.g. Nykjaer, 2009). From 1998 to 2019 the warming in the Ligurian Sea was +0.1208°C yr^{-1} (±0.0227) (Figure 12). In the equatorial Atlantic, the apparent rapid increase of temperature of +0.48 °C.yr^{-1} (±0.04) in 2005-2017 from the selected data indicated a change in water masses and circulation. The colder sea surface in 2005 was associated with the so-called Atlantic Cold Tongue (ACT) which was one of the most intense ATC since 1982 (Caniaux et al., 2011). The ACT also leads to significant changes in oceanic fCO_2 and air-sea CO_2 fluxes (Parard et al., 2010; Koseki et al., 2023) and explained the high C_T concentrations observed in 2005 in this region (Figure 12, Koffi et al., 2010).

Total alkalinity presents rather homogenous concentrations in the NASGP and the south Indian Ocean. Inter-annual variability of A_T is pronounced in the equatorial Atlantic ranging between 2245 and 2378 µmol kg^{-1}. This is mainly related to salinity as normalized A_T values (N-A_T, for salinity= 35) do not show such inter-annual variability (Mean N-A_T = 2295.7 ±4.6 µmol kg^{-1}, n= 67 for 2005-2017, not shown). In the coastal zones off Brittany, the A_T is also highly variable (Salt et al., 2016; Gac et al., 2021) ranging between 2150 and 2386 µmol kg^{-1} (Figure 12).

An interesting signal is the progressive increase of A_T in the Mediterranean Sea. The positive A_T trend of +0.53 (±0.11) µmol kg^{-1} yr^{-1} (n=538) in 1998-2019 in the region offshore was also observed at the coastal station SOMLIT-Point-B in 2007-2015 but with a faster increase of +2.08 (±0.19) µmol kg^{-1} yr^{-1} (Kapsenberg et al., 2017). Close to the DYFAMED site, at station SOMLIT-Point-B, the A_T trend was not linked to salinity temporal changes as a positive N-A_T trend was also reported, +0.52 (± 0.07) µmol kg^{-1} yr^{-1} (not shown). Based on data from the PERLE cruises in 2018-2021 a significant increase in A_T was also identified in the Eastern Mediterranean Sea (Wimart-Rousseau et al., 2021). Along with the increase of C_T and the warming, the A_T increase would impact on the fCO_2, air-sea CO_2 fluxes and pH temporal changes (Merlivat et al., 2018). Processes explaining the A_T increase in the Mediterranean Sea are still unexplained and deserve further investigations (Coppola et al., 2019).

As expected, because of the anthropogenic CO_2 uptake the C_T concentrations increased in most regions (Figure 12, Table 6). This is identified in the Indian Ocean (in the subtropics and the high latitude), in the Mediterranean Sea, and in coastal waters off Brittany. However, the signal is more complex in the NASPG. As previously shown the C_T trend in the NASPG depends on seasons and decades (Metzl et al., 2010; Reverdin et al., 2018; Fröb et al., 2019; Leseurre et al., 2020). Here we selected only the data in January-February from the SURATLANT cruises leading a C_T trend of +0.72 (±0.17) µmol kg^{-1} yr^{-1}. Compared to the regions further north the C_T trend in the NASPG is about half the C_T trends of +1.44 (±0.23) µmol kg^{-1} yr^{-1} observed in the Iceland Sea (Olafsson et al., 2009) or +1.48 (±0.22) µmol kg^{-1} yr^{-1} at station M in the Norwegian Sea (Skjelvan et al., 2022).

In the coastal zones off Brittany, although there are large seasonal and inter-annual variabilities (Gac et al., 2021), an annual C_T trend of +1.72 (±0.28) µmol kg^{-1} yr^{-1} is detected over 10 years (2009 to 2019). The same is observed in the Mediterranean Sea where the C_T offshore trend of +0.69 (±0.18) µmol kg^{-1} yr^{-1} is low compared to what was observed in the coastal zone (SOMLIT-Point-B, +2.97 (±0.20) µmol kg^{-1} yr^{-1}, Kapsenberg et al., 2017).

In the southern Indian Ocean, C_T concentrations also increased in both subtropical and high latitudes, two regions where the primary productivity is relatively low (oligotrophic regime in the subtropics and High Nutrient Low Chlorophyll regime, HNLC, south of the Polar Front). With the data selected for austral summer

(January-February) the C_T trends appeared almost similar in these two regions, around +0.65 µmol kg^{-1} yr^{-1} (Table 6).

Finally, in the Equatorial Atlantic the selected data around 0°-10°W highlighted the large variability linked to the oceanic circulation. Detecting a C_T trend as well as a possible link with anthropogenic carbon uptake, at least with the data available in 2005-2017, appears to be intricate as it has been previously discussed for the period 2006-2013 (Lefèvre et al., 2016). However, the signal of the C_T increase is better identified north or south of the Equator in the Eastern tropical Atlantic sector (Lefèvre et al., 2021).

In the water column A_T and C_T data from dedicated cruises were used to evaluate the anthropogenic CO_2 (C_{ant}) distribution and pH change since pre-industrial era (e.g. PANDORA cruise, Ganachaud et al., 2017; OUTPACE cruise, Wagener et al., 2018; SOMBA cruise, Keraghel et al., 2020). Time-series at DYFAMED station also enabled to investigate the temporal variability of C_T, A_T and C_{ant} in the water column (Touratier and Goyet, 2009; Coppola et al., 2020; Fourrier et al., 2022). As an example of the observed temporal variations at depth we selected the data in the layer 950-1050m in the Ligurian Sea from different cruises (Figure 13). At that depth both A_T and C_T present some large anomalies especially noticed in 2013 (lower A_T and C_T in February 2013, DEWEX cruise) and in 2018 (higher A_T and C_T in May 2018, MOOSE-GE cruise) the later probably linked to episodic convective process that occurred in winter 2018 (Fourrier et al., 2022; Coppola et al, 2023). During the strong convection event in 2013 the positive anomalies of A_T and C_T were mostly identified in the upper layers (Figure 12c).

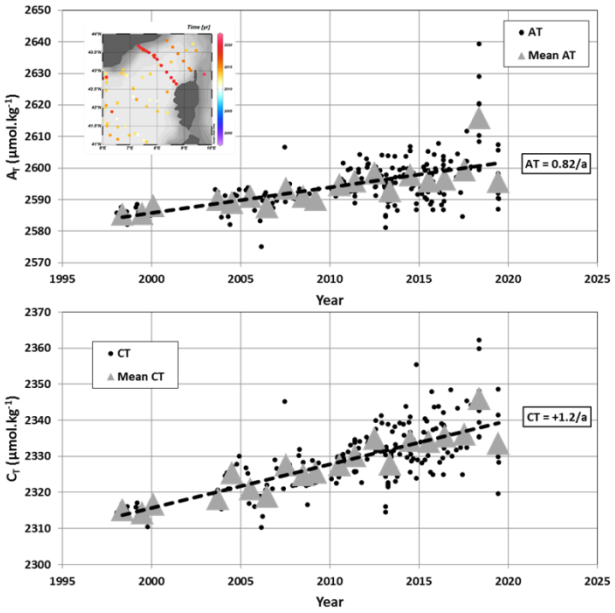

Figure 13: Time-series of A_T (µmol kg^{-1}) and C_T (µmol kg^{-1}) in the Ligurian Sea (1998-2019) in the layer 950-1050m. Annual mean (grey triangles) was calculated from all data each year (black dots). The trends (dashed line) based on annual mean are +0.82 (±0.15) µmol kg^{-1} yr^{-1} for A_T and +1.20 (±0.12) µmol kg^{-1} yr^{-1} for C_T. In this layer data selected are from cruises ANTARES, CASCADE, DEWEX, DYFAMED, MOOSE-GE and PEACETIME (location of stations shown in the inserted map).

In this region the long-term increase of A_T indicates that in addition to the anthropogenic CO_2 signal other processes are at play to explain the rapid C_T trend of +1.20 (±0.12) µmol kg^{-1} yr^{-1} at depth compared to that observed in surface (Figure 12). The signal at depth is probably linked to the variations of the deep convection and mixing with Levantine intermediate water (LIW, Margirier et al., 2020) with higher A_T and C_T

concentrations. The long-term increase of A_T and C_T at depth (here at 1000m, Figure 13) was also observed below 2000m (Coppola et al., 2020) a signal that has to be investigated in dedicated analysis using other properties (O_2, nutrients, following Fourrier et al. (2022) for the period 2012-2020) and a larger dataset in the Mediterranean Sea (e.g. GLODAP).

6 Using A_T and C_T data to validate observations from autonomous instruments

The dataset presented in this synthesis would also offer interesting observations to validate properties (A_T and C_T) derived from BGC-Argo floats equipped with pH sensors (e.g. Bushinsky et al., 2019; Mazloff et al., 2023; Mignot et al., 2023). The water column in situ A_T and C_T data obtained during the Antarctic Circumpolar Expedition (ACE) in 2016-2017 were collected at location where SOCCOM floats were launched (Walton and Thomas, 2018). A SOCCOM float (WMO ID 5905069) was launched on January 11th 2017 at 55°S-96°E south of the Polar Front in the southern Indian Ocean. The pH, temperature and salinity data from the float were then used to derive A_T and C_T profiles (here using a multiple linear regression (MLR) algorithm, Williams et al., 2016, 2017). In the top layers the discrete ACE data (Figure 14) present large variability of A_T and C_T concentrations not captured in the records derived from the float (MLR method somehow smooth the profiles). However, given the uncertainty in reconstructed A_T from float data (5.6 µmol kg^{-1}) the average values in the first 100m were almost identical (A_T-$_{ACE}$ = 2285.1 (±4.4) µmol kg^{-1} and A_T-$_{float}$ = 2278.3 (±0.7) µmol kg^{-1}; C_T-$_{ACE}$ = 2139.7 (±9.2) µmol kg^{-1} and C_T-$_{float}$ = 2141.1 (±3.2) µmol kg^{-1}). Moreover below 200m, profiles from the float are coherent compared to the A_T and C_T measurements (Figure 14). This is encouraging for using float data to explore the seasonal variability of A_T and C_T in the Southern Ocean (e.g. Williams et al., 2018; Johnson et al., 2022) and the estimation of anthropogenic CO_2 in the water column in this sector (Figure 14). Here the C_{ant} concentrations were calculated below 200m (corresponding to the temperature minimum of the winter winter in the SO and using the TrOCA method, Touratier et al., 2007). The float data suggest that C_{ant} concentrations are positive down to about 1000m, with maximum values in subsurface. In 2017 the mean C_{ant} concentration at 200m was 49.1 (±9.0) µmol kg^{-1}. Below that depth, C_{ant} decreased and reduced to +29.8 (±8.5) µmol kg^{-1} in the layer 300-400m. To complement the C_{ant} inventories based on GLODAP data product (e.g. Gruber et al., 2019) C_{ant} estimates derived from BGC-Argo floats as evaluated here in the Southern Ocean could be applied in other locations as was previously tested in the North Pacific (Li et al., 2019).

In surface water as the A_T derived from the float data are deduced using MLR or LIAR methods (Williams et al., 2017; Carter et al., 2016), the A_T data in the SNAPO-CO2 synthesis could also be used to identify A_T anomalies not always captured from floats. This is particularly relevant in coccolithophores blooms areas when low A_T concentrations and high pCO_2 are observed (e.g. Balch et al., 2016 in the Southern Ocean; Robertson et al., 1994 in the North Atlantic).

7 Summary and suggestions

The ocean data synthesized in this product are based on measurements of A_T and C_T performed between the period 1993 and 2022 with an accuracy of ±4 µmol kg^{-1}. It offers a large data set of A_T and C_T for the global ocean and regional biogeochemical studies. It includes more than 44 400 surface and water column observations in all oceanic basins, in the Mediterranean Sea, in the coastal zones, near coral reefs, and in rivers. For the open ocean this complements the SOCAT and GLODAP data products (Bakker et al., 2016; Lauvset et al., 2022). For

the coastal sites this also complements the synthesis of coastal time-series only done around North America (Fassbender et al., 2018; Jiang et al., 2021; OCADS, 2023).

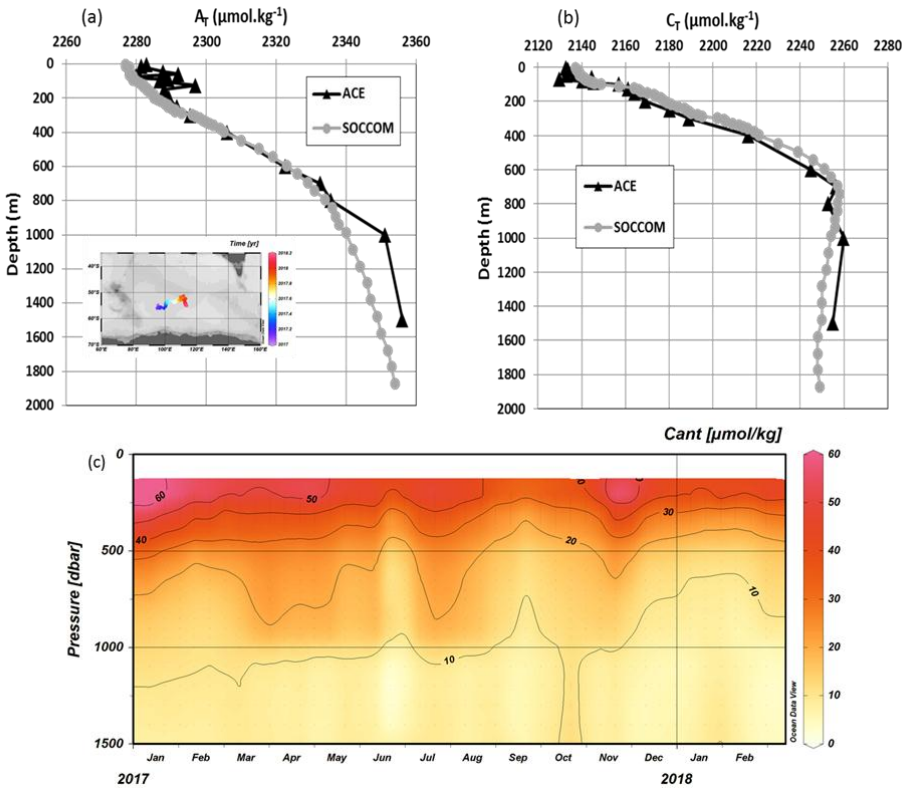

Figure 14: Profiles of (a) A_T (µmol kg^{-1}) and (b) C_T (µmol kg^{-1}) observed at station ACE-20 (55°S-95°E, 11/1/17, black triangles) compared with the profiles deduced from the SOCCOM float (WMO code 5905069) launched at that location (first data on January 12th 2017, grey circles). The location/drift of the float in 2017-2018 is shown on the inserted map. (c) Hovmoller section (Pressure/time) of anthropogenic CO_2 concentrations (C_{ant} in µmol kg^{-1}) estimated from the float data (A_T, C_T, O_2, T) below 200m (period January 2017-February 2018). Section produced with ODV (Schlitzer, 2018).

The SNAPO-CO2 dataset enables to investigate seasonal variations to decadal trends of A_T and C_T in various oceanic provinces. In regions where data are available for more than 2 decades in surface water (North Atlantic, Ligurian Sea, Southern Indian Ocean, and coastal regions), all time-series show an increase in C_T. Excepted in the Mediterranean Sea, A_T appears relatively constant over time, although the A_T content present significant inter-annual variability such as in the NASPG or in the coastal zones including near the Congo and Amazon Rivers plumes.

This dataset represents independent data for validation of reconstructed A_T or C_T fields using various methods (e.g. Rödenbeck et al., 2013, 2015; Sauzède et al., 2017; Turk et al., 2017; Bittig et al., 2018; Broullón et al., 2019, 2020; Land et al., 2019; Keppler et al., 2020; Fourier et al., 2020; Gregor and Gruber, 2021; Sims et al., 2023; Chau et al., 2023). It is also useful to validate Earth System Models (ESM) that currently present bias to reproduce the seasonal cycle of C_T and A_T due to inadequate representation of biogeochemical cycles, including the coupling of biological and physical processes (e.g. Pilcher et al., 2015; Mongwe et al., 2018; Lerner et al., 2021). This should be resolved for confident in future projections of the productivity, ocean acidification, and the responses of the marine ecosystems (e.g. Kwiatowkki et al., 2020). Recall that OBGM or ESM models calculate pCO_2 from A_T/C_T pairs and the simulated annual CO_2 flux might be correct when

compared to observations but for wrong reasons (e.g. Goris et al., 2018, Lerner et al., 2021). For example, it has been shown that biases in A_T in ESM models led to an overestimation of the oceanic fCO_2 trend and thus uncertainty when predicting the oceanic anthropogenic CO_2 uptake (Lebehot et al., 2019). The simulated seasonal cycle of fCO_2 is also uncertain in ESM models especially in high latitudes (e.g. Joos et al., 2023). It is thus important to attempt validating ESM models with A_T and C_T data such as presented in this synthesis.

This dataset would also serve for validating autonomous platforms capable of measuring pH and fCO_2 variables and, along with SOCAT and GLODAP datasets, provides an additional reference dataset for the development and validation of regional biogeochemical models for simulating air-sea CO_2 fluxes. It is also essential for training and validating neural networks capable of predicting variables in the carbonate system, thereby enhancing observations of marine CO_2 at different spatial and temporal scales.

The data presented here are available online on the Seanoe servor (Metzl et al., 2023, https://doi.org/10.17882/95414) and is divided in two files: one for the Global Ocean, and one for the Mediterranean Sea. The sources of the original datasets (doi) with the associated references are listed in the Supplementary Material (Table S3, S4). We invite the users to comment on any anomaly that would have not been detected or to suggest potential misqualification of data in the present product (e.g. data probably good although assigned with flag 3, probably wrong). The SNAPO-CO2 dataset will be regularly updated on Seanoe data servor with new observations controlled and archived.

8 Data availability

Data presented in this study are available at Seanoe: https://www.seanoe.org, https://doi.org/10.17882/95414 (Metzl et al., 2023).

Author contributions. NM prepared the data synthesis, the figures and wrote the draft of the manuscript with contributions from all authors. JF measured the discrete samples since 2014, with the help from CM and CLM, and prepared the individual reports for each project. NM and JF pre-qualified the discrete A_T/C_T data. CLM and NM are co-Is of the ongoing OISO project and qualified the underway A_T/C_T data from OISO and CLIM-EPARSES cruises. All authors have contributed either to organizing cruises, sample collection and/or data qualification, and reviewed the manuscript.

Competing interest. The authors declare that they have no conflict of interest.

Acknowledgments. The A_T and C_T data presented in this study were measured at the SNAPO-CO2 facility (Service National d'Analyse des Paramètres Océaniques du CO2) housed by the LOCEAN laboratory and part of the OSU ECCE Terra at Sorbonne University and INSU/CNRS analytical services. Support by INSU/CNRS, by OSU ECCE Terra and by LOCEAN, is gratefully acknowledged as well as support by different French "Services nationaux d'Observations", such as OISO/CARAUS, SOMLIT, PIRATA, SSS and MOOSE. We thank the research infrastructure ICOS (Integrated Carbon Observation System) France for funding a large part of the analyses. We thank the French oceanographic fleet ("Flotte océanographique française") for financial and logistic support for most cruises listed in this synthesis and for the OISO program (https://campagnes.flotteoceanographique.fr/series/228/). We acknowledge the MOOSE program (Mediterranean Ocean Observing System for the Environment, https://campagnes.flotteoceanographique.fr/series/235/fr/) coordinated by CNRS-INSU and the Research Infrastructure ILICO (CNRS-IFREMER). AWIPEV-CO2 was

supported by the Coastal Observing System for Northern and Arctic Seas (COSYNA), the two Helmholtz large-scale infrastructure projects ACROSS and MOSES, the French Polar Institute (IPEV) as well as the European Union's Horizon 2020 research and innovation projects Jericho-Next (No 871153 and 951799), INTAROS (No 727890) and FACE-IT (No 869154). The BOUSSOLE time series project was funded by the Centre National d'Etudes Spatiales (CNES) and the European Space Agency (ESA ESRIN contract 4000119096/17/I-BG), and the first three years of the CO2 time series at that site were funded by the French Agence Nationale de la Recherche (ANR). The EURECA4-OA cruise was also supported by the EUREC4A-OA JPI Ocean and Climate program. We thank Tara Ocean Foundation and many institutes and funding agencies for supporting TARA cruises since 2009. The OISO program was supported by the French institutes INSU (Institut National des Sciences de l'Univers) and IPEV (Institut Polaire Paul-Emile Victor), OSU Ecce-Terra (at Sorbonne Université), and the French program SOERE/Great-Gases. The CLIM-EPARSES cruise was supported by TAAF (Terres Australes et ANtarctiques Françaises), Fondation du Prince Albert II de Monaco, IRD, OSU Ecce-Terra, CNRS, MNHN, LOCEAN and LSCE laboratory. Data from the float launched during the ACE cruise were made freely available by the Southern Ocean Carbon and Climate Observations and Modeling (SOCCOM) Project funded by the National Science Foundation, Division of Polar Programs (NSF PLR -1425989), supplemented by NASA, and by the International Argo Program and the NOAA programs that contribute to it. The Argo Program is part of the Global Ocean Observing System (http://doi.org/10.17882/42182, http://argo.jcompos.org). We thank Frédéric Merceur (IFREMER) for preparing the page and data availability on Seanoe. We thank Patrick Raimbault (retired, former at MIO, Marseille) for managing the MOOSE project until 2019. We thank all colleagues and students who participated to the cruises and have carefully collected the precious seawater samples. We warmly acknowledge our colleague Christian Brunet (retired) for his supportive help for the analysis since the start of the Service facility SNAPO-CO2. We would like to pay tribute to our late colleague Frédéric Diaz who contributed to the LATEX cruise in 2010. We thank the associated editor Xingchen Wang to manage this manuscript, Marta Álvarez and a (more or less) anonymous reviewer for their suggestions that helped to improve this article.

References

Álvarez, M., Catalá, T. S., Civitarese, G., Coppola, L., Hassoun, A. E.R., Ibello, V., Lazzari, P., Lefevre, D., Macías, D., Santinelli, C. and Ulses, C.: Chapter 11 - Mediterranean Sea general biogeochemistry, Editor(s): Katrin Schroeder, Jacopo Chiggiato, Oceanography of the Mediterranean Sea, Elsevier, Pages 387-451, https://doi.org/10.1016/B978-0-12-823692-5.00004-2., 2023.

Bakker, D. C. E., Pfeil, B., Smith, K., Hankin, S., Olsen, A., Alin, S. R., Cosca, C., Harasawa, S., Kozyr, A., Nojiri, Y., O'Brien, K. M., Schuster, U., Telszewski, M., Tilbrook, B., Wada, C., Akl, J., Barbero, L., Bates, N. R., Boutin, J., Bozec, Y., Cai, W.-J., Castle, R. D., Chavez, F. P., Chen, L., Chierici, M., Currie, K., De Baar, H. J. W., Evans, W., Feely, R. A., Fransson, A., Gao, Z., Hales, B., Hardman-Mountford, N. J., Hoppema, M., Huang, W.-J., Hunt, C. W., Huss, B., Ichikawa, T., Johannessen, T., Jones, E. M., Jones, S., Jutterstrøm, S., Kitidis, V., Körtzinger, A., Landschützer, P., Lauvset, S. K., Lefèvre, N., Manke, A. B., Mathis, J. T., Merlivat, L., Metzl, N., Murata, A., Newberger, T., Omar, A. M., Ono, T., Park, G.-H., Paterson, K., Pierrot, D., Ríos, A. F., Sabine, C. L., Saito, S., Salisbury, J., Sarma, V. V. S. S., Schlitzer, R., Sieger, R., Skjelvan, I., Steinhoff, T., Sullivan, K. F., Sun, H., Sutton, A. J., Suzuki, T., Sweeney, C., Takahashi, T., Tjiputra, J., Tsurushima, N., Van Heuven, S. M. A. C., Vandemark, D., Vlahos, P., Wallace, D. W. R., Wanninkhof, R. and Watson, A. J.: An update to the Surface Ocean CO_2 Atlas (SOCAT version 2). Earth System Science Data, 6, 69-90. doi:10.5194/essd-6-69-2014. 2014

Bakker, D. C. E., Pfeil, B., Landa, C. S., Metzl, N., O'Brien, K. M., Olsen, A., Smith, K., Cosca, C., Harasawa, S., Jones, S. D., Nakaoka, S.-I., Nojiri, Y., Schuster, U., Steinhoff, T., Sweeney, C., Takahashi, T., Tilbrook, B., Wada, C., Wanninkhof, R., Alin, S. R., Balestrini, C. F., Barbero, L., Bates, N. R., Bianchi, A. A., Bonou, F., Boutin, J., Bozec, Y., Burger, E. F., Cai, W.-J., Castle, R. D., Chen, L., Chierici, M., Currie, K., Evans, W., Featherstone, C., Feely, R. A., Fransson, A., Goyet, C., Greenwood, N., Gregor, L., Hankin, S., Hardman-Mountford, N. J., Harlay, J., Hauck, J., Hoppema, M., Humphreys, M. P., Hunt, C. W., Huss, B., Ibánhez, J. S. P., Johannessen, T., Keeling, R., Kitidis, V., Körtzinger, A., Kozyr, A., Krasakopoulou, E., Kuwata, A., Landschützer, P., Lauvset, S. K., Lefèvre, N., Lo Monaco, C., Manke, A., Mathis, J. T., Merlivat, L., Millero, F. J., Monteiro, P. M. S., Munro, D. R., Murata, A., Newberger, T., Omar, A. M., Ono, T., Paterson, K., Pearce, D., Pierrot, D., Robbins, L. L., Saito, S., Salisbury, J., Schlitzer, R., Schneider, B., Schweitzer, R., Sieger, R., Skjelvan, I., Sullivan, K. F., Sutherland, S. C., Sutton, A. J., Tadokoro, K., Telszewski, M., Tuma, M., Van Heuven, S. M. A. C., Vandemark, D., Ward, B., Watson, A. J., and Xu, S.: A multi-decade record of high-quality fCO_2 data in version 3 of the Surface Ocean CO_2 Atlas (SOCAT), Earth Syst. Sci. Data, 8, 383-413, doi:10.5194/essd-8-383-2016. 2016.

Bakker, D.C.E., Alin, S.R., Bates, N.R., Becker, M., Feely, R. A., Gritzalis, T. , Jones, S. D., Kozyr, A., Lauvset, S. K., Metzl, N., Munro, D.R., Nakaoka, S.–I., Nojiri, Y., O'Brien, K., Olsen, A., Pierrot, D., Rehder, G., Steinhoff, T., Sutton, A., Sweeney, C., Tilbrook, B., Wada, C., Wanninkhof, R., and all >100 SOCAT contributors: An alarming decline in the ocean CO_2 observing capacity. Available at www.socat.info, 2023.

Balch, W.M., Bates, N.R., Lam, P.J., Twining, B.S., Rosengard, S. Z., Bowler, B.C., Drapeau, D.T., Garley, R., Lubelczyk, L.C., Mitchell, C. and Rauschenberg S.: Factors regulating the Great Calcite Belt in the Southern Ocean and its biogeochemical significance. Global Biogeochem. Cycles, 30, doi:10.1002/2016GB005414, 2016

Beaufort, L., Probert, I., de Garidel-Thoron, T., Bendif, E.M., Ruiz-Pino, D., Metzl, N., Goyet, C., Buchet, N., Coupel, P., Grelaud, M., Rost, B., Rickaby, R.E.M., and de Vargas C.: Sensitivity of coccolithophores to carbonate chemistry and ocean acidification. *Nature*, doi:10.1038/nature10295. 2011

Bittig, H.C., Steinhoff, T., Claustre, H., Fiedler, B., Williams, N.L., Sauzède, R., Körtzinger, A. and Gattuso, J.-P.: An Alternative to Static Climatologies: Robust Estimation of Open Ocean CO2 Variables and Nutrient Concentrations From T, S, and O2 Data Using Bayesian Neural Networks. Front. Mar. Sci. 5:328. doi: 10.3389/fmars.2018.00328, 2018

Bockmon, E. E., and Dickson, A. G.,: An inter-laboratory comparison assessing the quality of seawater carbon dioxide measurements. *Marine Chemistry*, *171*, *36-43*, doi:10.1016/j.marchem.2015.02.002, 2015.

Bosse, A., Testor, P., Mayot, N., Prieur, L., D'Ortenzio, F., Mortier, L., Le Goff, H., Gourcuff, C., Coppola, L., Lavigne, H. and Raimbault, P.: A submesoscale coherent vortex in the Ligurian Sea: From dynamical barriers to biological implications. *J. Geophys. Res. Oceans*, *122*, doi:10.1002/2016JC012634., 2017.

Bozec, Y., Merlivat, L., Baudoux, A.-C., Beaumont, L., Blain, S., Bucciarelli, E., Danguy, T., Grossteffan, E., Guillot, A., Guillou, J., Répécaud, M., and Tréguer, P.: Diurnal to inter-annual dynamics of pCO_2 recorded by a CARIOCA sensor in a temperate coastal ecosystem (2003–2009). Marine Chemistry, 126, 1-4, 13-26, 10.1016/j.marchem.2011.03.003. 2011

Broullón, D., Pérez, F. F., Velo, A., Hoppema, M., Olsen, A., Takahashi, T., Key, R. M., Tanhua, T., González-Dávila, M., Jeansson, E., Kozyr, A., and van Heuven, S. M. A. C.: A global monthly climatology of total alkalinity: a neural network approach, Earth Syst. Sci. Data, 11, 1109–1127, https://doi.org/10.5194/essd-11-1109-2019. 2019

Broullón, D., Pérez, F. F., Velo, A., Hoppema, M., Olsen, A., Takahashi, T., Key, R. M., Tanhua, T., Santana-Casiano, J. M., and Kozyr, A.: A global monthly climatology of oceanic total dissolved inorganic carbon: a neural network approach, Earth Syst. Sci. Data, 12, 1725–1743, https://doi.org/10.5194/essd-12-1725-2020. 2020

Bushinsky, S. M., Landschützer, P., Rödenbeck, C., Gray, A. R., Baker, D., Mazloff, M. R., Resplandy L., Johnson K. S., and Sarmiento, J. L.: Reassessing Southern Ocean air-sea CO_2 flux estimates with the addition of biogeochemical float observations. Global Biogeochemical Cycles, 33. doi: 10.1029/2019GB006176, 2019.

Canesi, M., Douville, E., Montagna, P., Taviani, M., Stolarski, J., Bordier, L., Dapoigny, A., Coulibaly, G. E. H., Simon, A.-C., Agelou, M., Fin, J., Metzl, N., Iwankow, G., Allemand, D., Planes, S., Moulin, C., Lombard, F., Bourdin, G., Troublé, R., Agostini, S., Banaigs, B., Boissin, E., Boss, E., Bowler, C., de Vargas, C., Flores, M., Forcioli, D., Furla, P., Gilson, E., Galand, P. E., Pesant, S., Sunagawa, S., Thomas, O., Thurber, R. V., Voolstra, C. R., Wincker, P., Zoccola, D., and Reynaud, S.: Differences in carbonate chemistry up-regulation of long-lived reef-building corals. Sci. Rep. 13, 11589, Doi: 10.1038/s41598-023-37598-9, 2023.

Caniaux, G., Giordani, H., Redelsperger, J-L., Guichard, F., Key, E. and Wade, M.: Coupling between the Atlantic cold tongue and the West African monsoon in boreal spring and summer. J. Geophys. Res., 119, C04003, doi:10.1029/2010JC006570., 2011.

Cariou, T., and Bozec, Y.: COMOR-CARBORHONE 1 cruise, RV L'Europe, https://doi.org/10.17600/11060060, 2011a.

Cariou, T., and Bozec, Y.: COMOR-CARBORHONE 2 cruise, RV Téthys II, https://doi.org/10.17600/11450150, 2011b.

Cariou, T., and Bozec, Y.: CARBORHONE 3 cruise, RV Téthys II, https://doi.org/10.17600/12450020, 2012a.

Cariou, T., and Bozec Y.: CARBORHONE 4 cruise, RV Téthys II, https://doi.org/10.17600/12450140, 2012b.

Carter, B. R., Williams, N. L., Gray, A. R., and Feely, R. A.: Locally interpolated alkalinity regression for global alkalinity estimation, Limnol. Oceanogr. Methods, 14(4), 268–277, doi:10.1002/lom3.10087, 2016.

Chen, H., Haumann, F. A., Talley, L. D., Johnson, K. S., and Sarmiento, J. L.: The deep ocean's carbon exhaust. Global Biogeochemical Cycles. doi: https://doi.org/10.1002/essoar.10507757.1, 2022

Cheng, L. J., Abraham, J., Zhu, J., Trenberth, K. E., Fasullo, J., Boyer, T., Locarnini, R., Zhang, B., Yu, F. J., Wan, L. Y., Chen, X. R., Song, X. Z., Liu, Y. L., and Mann, M. E.: Record-setting ocean warmth continued in 2019, Adv. Atmos. Sci, 37, 137-142. https://doi.org/10.1007/s00376-020-9283-7, 2020

Claustre, H., Johnson, K. S., and Takeshita, Y.**:** Observing the Global Ocean with Biogeochemical-Argo. Annual Review of Marine Science, 12: 23-48 | DOI: 10.1146/annurev-marine-010419-010956,2020.

Conan, P., Guieux, A., and Vuillemin, R.: MOOSE (MOLA), https://doi.org/10.18142/234, 2020.

Copin-Montégut, C.: Alkalinity and carbon budgets in the Mediterranean Sea, Global Biogeochemical Cycles, vol. 7, pp. 915–925, 1993.

Copin-Montégut, C., and Bégovic, M.: Distributions of carbonate properties and oxygen along the water column (0–2000 m) in the central part of the NW Mediterranean Sea (Dyfamed site): influence of the winter vertical mixing on air–sea CO2 and O2 exchanges. Deep-Sea Research II 49, 2049–2066, https://doi.org/10.1016/S0967-0645(02)00027-9,2002.

Coppola, L., and Diamond-Riquier, E,: MOOSE (DYFAMED), https://doi.org/10.18142/131, 2008.

Coppola, L., Raimbault, P., Mortier, L., and Testor, P.: Monitoring the environment in the northwestern Mediterranean Sea, Eos, 100, https://doi.org/10.1029/2019EO125951. Published on 25 July 2019.

Coppola, L., Boutin, J., Gattuso, J.-P., Lefèvre, D., and Metzl, N.: The Carbonate System in the Ligurian Sea. In *The Mediterranean Sea in the Era of Global Change: Evidence from 30 years of multidisciplinary study of the Ligurian Sea*, C. Migon, P. Nival, A. Sciandra, Eds. (ISTE Science Publishing LTD, London, UK, 2020), vol. 1, chap. 4, pp. 79-104. ISBN: 9781786304285. https://doi.org/10.1002/9781119706960.ch4, 2020.

Coppola, L., Fourrier, M., Pasqueron de Fommervault, O., Poteau, A., Riquier, E. D. and Béguery, L.: Highresolution study of the air-sea CO2 flux and net community oxygen production in the Ligurian Sea by a fleet of gliders. Front. Mar. Sci. 10:1233845. doi: 10.3389/fmars.2023.1233845, 2023

Corbière, A., Metzl, N., Reverdin, G., Brunet, C., and Takahashi, T.: Interannual and decadal variability of the oceanic carbon sink in the North Atlantic subpolar gyre**.** *Tellus B*, Vol. 59, issue 2, 168-179, DOI: 10.1111/j.1600-0889.2006.00232, 2007.

D'Ortenzio, F. and Taillandier, V: BIO-ARGO-MED-2018 cruise, RV Téthys II, https://doi.org/10.17600/18000550, 2018.

De Carlo, E. H., Mousseau, L., Passafiume, O., Drupp, P. and Gattuso J.-P.: Carbonate chemistry and air-sea CO_2 flux in a NW Mediterranean bay over a four-year period: 2007-2011. *Aquatic Geochemistry* doi:10.1007/s10498-013-9217-4, 2013.

Dickson, A. G., Sabine, C. L., and Christian, J. R.: Guide to best practices for ocean CO2 measurements, North Pacific Marine Science Organization, Sidney, British Columbia, 191, https://doi.org/10.25607/OBP-1342, 2007.

Division Plans de DMI – SHOM : PROTEUS2010_LEG1 cruise, RV Pourquoi pas ?, https://doi.org/10.17600/10030040, 2010.

Division Plans de DMI – SHOM: PROTEVSMED_PERLE_2018 cruise, RV L'Atalante, https://campagnes.flotteoceanographique.fr/campaign, 2018.

Doney, S. C., Fabry, V. J., Feely, R. A., and Kleypas, J. A., Ocean acidification: The other CO2 problem. *Annual Review of Marine Science*, 1(1), 169–192. 10.1146/annurev.marine.010908.163834, 2009

Doney, S. C., Busch, D. S., Cooley, S. R., and Kroeker, K. J.: The Impacts of Ocean Acidification on Marine Ecosystems and Reliant Human Communities. Annual Review of Environment and Resources 45:1, https://doi.org/10.1146/annurev-environ-012320-083019. 2020

Douville, E., Bourdin, G., Lombard, F., Gorsky, G., Fin, J., Metzl, N., Pesant, S., and Tara Pacific Consortium: Seawater carbonate chemistry dataset collected during the Tara Pacific Expedition 2016-2018. PANGAEA, https://doi.org/10.1594/PANGAEA.944420, 2022.

Durrieu de Madron, X.: CASCADE cruise, RV L'Atalante, https://doi.org/10.17600/11010020, 2011.

Durrieu de Madron, X., and Conan, P.: PERLE2 cruise, RV Pourquoi pas ?, https://doi.org/10.17600/18000865, 2018

Edmond, J. M.: High precision determination of titration alkalinity and total carbon dioxide content of sea water by potentiometric titration, Deep-Sea Res., 17, 737–750, https://doi.org/10.1016/0011-7471(70)90038-0, 1970.

Eldin, G. : PANDORA cruise, RV L'Atalante, https://doi.org/10.17600/12010050, 2012.

Eyring, V., Righi, M., Lauer, A., Evaldsson, M., Wenzel, S., Jones, C., Anav, A., Andrews, O., Cionni, I., Davin, E. L., Deser, C., Ehbrecht, C., Friedlingstein, P., Gleckler, P., Gottschaldt, K.-D., Hagemann, S., Juckes, M., Kindermann, S., Krasting, J., Kunert, D., Levine, R., Loew, A., Mäkelä, J., Martin, G., Mason, E., Phillips, A. S., Read, S., Rio, C., Roehrig, R., Senftleben, D., Sterl, A., van Ulft, L. H., Walton, J., Wang, S., and Williams, K.

D.: ESMValTool (v1.0) – a community diagnostic and performance metrics tool for routine evaluation of Earth system models in CMIP, Geosci. Model Dev., 9, 1747-1802, doi:10.5194/gmd-9-1747-2016, 2016.

Fabry, V. J., Seibel, B. A., Feely, R. A. and Orr, J. C.: Impacts of ocean acidification on marine fauna and ecosystem processes. *ICES J. Mar. Sci.* 65, 414–432. https://doi.org/10.1093/icesjms/fsn048, 2008.

Fassbender, A. J., Sabine, C. L., and Palevsky, H. I.: Nonuniform ocean acidification and attenuation of the ocean carbon sink, Geophys. Res. Lett., 44, 8404–8413, doi:10.1002/2017GL074389., 2017.

Fassbender, A. J., Alin, S. R., Feely, R. A., Sutton, A. J., Newton, J. A., Krembs, C., Bos, J., Keyzers, M., Devol, A., Ruef, W., and Pelletier, G.: Seasonal carbonate chemistry variability in marine surface waters of the US Pacific Northwest, Earth Syst. Sci. Data, 10, 1367–1401, https://doi.org/10.5194/essd-10-1367-2018, 2018.

Feely, R. A., Sabine, C. L., Byrne, R. H., Millero, F. J., Dickson, A. G., Wanninkhof, R., et al.: Decadal changes in the aragonite and calcite saturation state of the Pacific Ocean. Global Biogeochemical Cycles, 26, GB3001. https://doi.org/10.1029/2011GB004157, 2012.

Feely, R. A., Jiang, L.-Q., Wanninkhof, R., Carter, B. R., Alin, S. R., Bednaršek, N., and Cosca, C. E.: Acidification of the global surface ocean: What we have learned from observations. Oceanography, https://doi.org/10.5670/oceanog.2023.222, 2023

Fleury, E., Petton, S., Benabdelmouna, A., and Pouvreau, S., (coord.): Observatoire national du cycle de vie de l'huître creuse en France. Rapport annuel ECOSCOPA 2022. R.INT.BREST RBE/PFOM/PI 2023-1, 2023.

Fourrier, M., Coppola, L., Claustre, H., D'Ortenzio, F., Sauzède, R. and Gattuso, J.-P.: A regional neural network approach to estimate water-column nutrient concentrations and carbonate system variables in the Mediterranean Sea: CANYON-MED. Frontiers in Marine Science, 7:620, https://www.frontiersin.org/articles/10.3389/fmars.2020.00620, 2020.

Fourrier, M., Coppola, L., D'Ortenzio, F., Migon, C., and Gattuso, J.-P.: Impact of intermittent convection in the northwestern Mediterranean Sea on oxygen content, nutrients, and the carbonate system. Journal of Geophysical Research: Oceans, 127, e2022JC018615. https://doi.org/10.1029/2022JC018615, 2022

Friedlingstein, P., O'Sullivan, M., Jones, M. W., Andrew, R. M., Gregor, L., Hauck, J., Le Quéré, C., Luijkx, I. T., Olsen, A., Peters, G. P., Peters, W., Pongratz, J., Schwingshackl, C., Sitch, S., Canadell, J. G., Ciais, P., Jackson, R. B., Alin, S. R., Alkama, R., Arneth, A., Arora, V. K., Bates, N. R., Becker, M., Bellouin, N., Bittig, H. C., Bopp, L., Chevallier, F., Chini, L. P., Cronin, M., Evans, W., Falk, S., Feely, R. A., Gasser, T., Gehlen, M., Gkritzalis, T., Gloege, L., Grassi, G., Gruber, N., Gürses, Ö., Harris, I., Hefner, M., Houghton, R. A., Hurtt, G. C., Iida, Y., Ilyina, T., Jain, A. K., Jersild, A., Kadono, K., Kato, E., Kennedy, D., Klein Goldewijk, K., Knauer, J., Korsbakken, J. I., Landschützer, P., Lefèvre, N., Lindsay, K., Liu, J., Liu, Z., Marland, G., Mayot, N., McGrath, M. J., Metzl, N., Monacci, N. M., Munro, D. R., Nakaoka, S.-I., Niwa, Y., O'Brien, K., Ono, T., Palmer, P. I., Pan, N., Pierrot, D., Pocock, K., Poulter, B., Resplandy, L., Robertson, E., Rödenbeck, C., Rodriguez, C., Rosan, T. M., Schwinger, J., Séférian, R., Shutler, J. D., Skjelvan, I., Steinhoff, T., Sun, Q., Sutton, A. J., Sweeney, C., Takao, S., Tanhua, T., Tans, P. P., Tian, X., Tian, H., Tilbrook, B., Tsujino, H., Tubiello, F., van der Werf, G. R., Walker, A. P., Wanninkhof, R., Whitehead, C., Willstrand Wranne, A., Wright, R., Yuan, W., Yue, C., Yue, X., Zaehle, S., Zeng, J., and Zheng, B.: Global Carbon Budget 2022, Earth Syst. Sci. Data, 14, 4811–4900, https://doi.org/10.5194/essd-14-4811-2022, 2022.

Fröb, F., Olsen, A., Becker, M., Chafik, L., Johannessen, T., Reverdin, G., and Omar, A.: Wintertime fCO2 variability in the subpolar North Atlantic since 2004. Geophysical Research Letters, 46, https://doi.org/10.1029/2018GL080554, 2019.

Gac, J-P., Marrec, P., Cariou, T., Guillerm, C., Macé, E., Vernet, M., and Bozec, Y.: Cardinal buoys: An opportunity for the study of air-sea CO2 fluxes in coastal ecosystems. Front. Mar. Sci. doi: 10.3389/fmars.2020.00712. 2020.

Gac, J.-P., Marrec, P., Cariou, T., Grosstefan, E., Macé, E., Rimmelin-Maury, P., Vernet, M., and Bozec, Y.: Decadal Dynamics of the CO2 System and Associated Ocean Acidification in Coastal Ecosystems of the North East Atlantic Ocean. Front. Mar. Sci. 8:688008. doi:10.3389/fmars.2021.688008, 2021.

Ganachaud, A., Cravatte, S., Sprintall, J., Germineaud, C., Alberty, M., Jeandel, C., Eldin, G., Metzl, N., Bonnet, S., Benavides, M., Heimburger, L.-E, Lefèvre, J., Michael, S., Resing, J., Quéroué, F., Sarthou, G., Rodier, M., Berthelot, H., Baurand, F., Grelet, J., Hasegawa, T., Kessler, W., Kilepak, M., Lacan, F., Privat, E., Send, U., Van Beek, P., Souhaut, M. and Sonke, J. E.:. The Solomon Sea: its circulation, chemistry, geochemistry and biology explored during two oceanographic cruises. Elem Sci Anth, 5: 33, DOI: https://doi.org/10.1525/elementa.221, 2017.

Gattuso, J.-P., Magnan, A., Billé, R., Cheung, W. W. L., Howes, E. L., Joos, F., Allemand, D., Bopp, L., Cooley, S., Eakin, M., Hoegh-Guldberg, O., Kelly, R. P., Pörtner, H.-O., Rogers, A. D., Baxter, J. M., Laffoley, D., Osborn, D., Rankovic, A., Rochette, J., Sumaila, U. R., Treyer, S., and Turley, C.: Contrasting futures for ocean and society from different anthropogenic CO_2 emissions scenarios. *Science* 349:aac4722.doi: 10.1126/science.aac4722, 2015.

Gattuso, J.-P., Alliouane, S., and Mousseau, L.: Seawater carbonate chemistry in the Bay of Villefranche, Point B (France), January 2007 - September 2020. PANGAEA, https://doi.org/10.1594/PANGAEA.727120, 2021.

Gattuso, J.-P., Alliouane, S., and Fischer, P.: High-frequency, year-round time series of the carbonate chemistry in a high-Arctic fjord (Svalbard), Earth Syst. Sci. Data, 15, 2809–2825, https://doi.org/10.5194/essd-15-2809-2023, 2023.

Gattuso, J.–P., Alliouane, S., and Fischer, P.: High-frequency, year-round time series of the carbonate chemistry in a high-Arctic fjord (Svalbard) v2. PANGAEA, https://doi.org/10.1594/PANGAEA.960131, 2023.

Gemayel, E., Hassoun, A. E. R., Benallal, M. A., Goyet, C., Rivaro, P., Abboud-Abi Saab, M. , Krasakopoulou, E., Touratier, F. , and Ziveri, P.: Climatological variations of total alkalinity and total inorganic carbon in the Mediterranean Sea surface waters. Earth Syst. Dynam., 6, 789-800, doi:10.5194/esd-6-789-2015. 2015.

Golbol, M., Vellucci, V., and Antoine, D.: BOUSSOLE, https://doi.org/10.18142/1, 2000.

Golbol M., Boutin J., Merlivat L., Vellucci, V., and Antoine, D.: Dissolved Inorganic Carbon and Total Alkalinity sampled at Boussole site in the Medditerranean Sea. SEANOE. https://doi.org/10.17882/71911, 2020.

Goris, N., Tjiputra, J. F., Olsen, A., Schwinger, J., Lauvset, S. K. and Jeansson, E.: Constraining projection-based estimates of the future North Atlantic carbon uptake, J. Climate, 31, 3959–3978, https://doi.org/10.1175/JCLI-D-17-0564.1,2018.

Goyet, C., Beauverger, C., Brunet, C., and Poisson, A.: Distribution of carbon dioxide partial pressure in surface waters of the Southwest Indian Ocean, Tellus B: Chemical and Physical Meteorology, 43:1, 1-11, DOI: 10.3402/tellusb.v43i1.15242, 1991.

Gregor, L. and Gruber, N.: OceanSODA-ETHZ: a global gridded data set of the surface ocean carbonate system for seasonal to decadal studies of ocean acidification, Earth Syst. Sci. Data, 13, 777–808, https://doi.org/10.5194/essd-13-777-2021, 2021.

Gruber, N., Clement, D. , Carter, B. R., Feely, R. A., van Heuven, S., Hoppema, M., Ishii, M., Key, R. M., Kozyr, A., Lauvset, S. K., Lo Monaco, C. , Mathis, J. T., Murata, A., Olsen, A., Perez, F. F., Sabine, C. L., Tanhua, T., and Wanninkhof, R.: The oceanic sink for anthropogenic CO_2 from 1994 to 2007, Science vol. 363 (issue 6432), pp. 1193-1199. DOI: 10.1126/science.aau5153, 2019.

Guieu, C., Desboeufs, K., Albani, S., et al.: BIOGEOCHEMICAL dataset collected during the PEACETIME cruise. SEANOE. https://doi.org/10.17882/75747, 2020.

Hagens, M., and Middelburg, J. J.: Attributing seasonal pH variability in surface ocean waters to governing factors, Geophys. Res. Lett., 43, doi:10.1002/2016GL071719. 2016.

Henson, S. A., Painter, S. C., Holliday, N. P., Stinchcombe, M. C., and Giering, S. L. C.: Unusual subpolar North Atlantic phytoplankton bloom in 2010: Volcanic fertilization or North Atlantic Oscillation?, J. Geophys. Res. Oceans, 118, 4771–4780, doi:10.1002/jgrc.20363, 2013.

Hoegh-Guldberg, O., Mumby, P.J., Hooten, A.J., Steneck, R.S., Greenfield, P., Gomez, E., Harvell, C.D., Sale, P.F., Edwards, A.J., Caldeira, K., Knowlton, N., Eakin, C.M., Iglesias-Prieto, R., Muthiga, N., Bradbury, R.H., Dubi, A., and Hatziolos, M.E.: Coral reefs under rapid climate change and ocean acidification. Science 14, 1737–1742. https://doi.org/10.1126/science.1152509, 2007.

Hood, E.M., and Merlivat, L.: Annual to interannual variations of fCO(2) in the northwestern Mediterranean Sea: Results from hourly measurements made by CARIOCA buoys, 1995-1997, Journal Of Marine Research, 59, 113-131, doi: 10.1357/002224001321237399. 2001

Howes, E., Stemmann, L., Assailly, C., Irisson, J.-O., Dima, M., Bijma, J., Gattuso, J.-P.: Pteropod time series from the North Western Mediterranean (1967-2003): impacts of pH and climate variability. Mar Ecol Prog Ser 531: 193-206, doi: 10.3354/meps11322. 2015.

Howes, E. L., Eagle, R., Gattuso, J.-P., and Bijma, J.: Comparison of Mediterranean pteropod shell biometrics and ultrastructure from historical (1910 and 1921) and present day (2012) samples provides baseline for monitoring effects of global change. *PLoS ONE* 12:e0167891. 2017.

IPCC. Changing Ocean, Marine Ecosystems, and Dependent Communities. in The Ocean and Cryosphere in a Changing Climate 447–588 (Cambridge University Press, 2022). doi:10.1017/9781009157964.007. 2022

Jiang, Z.-P., Tyrrell, T., Hydes, D. J., Dai, M., and Hartman, S. E.: Variability of alkalinity and the alkalinity-salinity relationship in the tropical and subtropical surface ocean, Global Biogeochem. Cycles, 28, 729–742, doi:10.1002/2013GB004678, 2014.

Jiang, L.-Q., Feely, R. A., Carter, B. R., Greeley, D. J., Gledhill, D. K., and Arzayus K. M.: Climatological distribution of aragonite saturation state in the global oceans, Global Biogeochem. Cycles, 29, 1656–1673, doi:10.1002/2015GB005198, 2015.

Jiang, L.-Q., Carter, B. R., Feely, R. A., Lauvset, S. K. and Olsen, A.: Surface ocean pH and buffer capacity: past, present and future, *Sci Rep*, 9(1), 1–11, doi:10.1038/s41598-019-55039-4. 2019.

Jiang, L.-Q., Feely, R. A., Wanninkhof, R., Greeley, D., Barbero, L., Alin, S., Carter, B. R., Pierrot, D., Featherstone, C., Hooper, J., Melrose, C., Monacci, N., Sharp, J. D., Shellito, S., Xu, Y.-Y., Kozyr, A., Byrne, R. H., Cai, W.-J., Cross, J., Johnson, G. C., Hales, B., Langdon, C., Mathis, J., Salisbury, J., and Townsend, D. W.: Coastal Ocean Data Analysis Product in North America (CODAP-NA) – an internally consistent data product for discrete inorganic carbon, oxygen, and nutrients on the North American ocean margins. Earth System Science Data, 13(6), 2777–2799. https://doi.org/10.5194/essd-13-2777-2021, 2021

Jiang, L.-Q., Dunne, J., Carter, B. R., Tjiputra, J. F., Terhaar, J., Sharp, J. D., et al.: Global surface ocean acidification indicators from 1750 to 2100. Journal of Advances in Modeling Earth Systems, 15, e2022MS003563. https://doi.org/10.1029/2022MS003563 , 2023a

Jiang, L.Q., Kozyr, A., Relph, J.M. *et al.* The Ocean Carbon and Acidification Data System. Sci Data 10, 136. https://doi.org/10.1038/s41597-023-02042-0, 2023b

Johnson, K. S., Mazloff, M. R., Bif, M. B., Takeshita, Y., Jannasch, H. W., Maurer, T. L., et al.: Carbon to nitrogen uptake ratios observed across the Southern Ocean by the SOCCOM profiling float array. Journal of Geophysical Research: Oceans, 127, e2022JC018859. https://doi.org/10.1029/2022JC018859, 2022.

Joos, F., Hameau, A., Frölicher, T. L., and Stephenson, D. B.: Anthropogenic attribution of the increasing seasonal amplitude in surface ocean pCO2. Geophysical Research Letters, 50, e2023GL102857. https://doi.org/10.1029/2023GL102857, 2023.

Joyce, T. and Corry, C., eds: Requirements for WOCE Hydrographic Programme Data Reporting. WHPO Publication 90-1 Revision 2, WOCE Report 67/91, Woods Hole, Mass., USA, May 1994.

Kapsenberg, L., Alliouane, S., Gazeau, F., Mousseau, L., and Gattuso, J.-P.: Coastal ocean acidification and increasing total alkalinity in the northwestern Mediterranean Sea, Ocean Sci., 13, 411-426, doi:10.5194/os-13-411-2017, 2017.

Keppler, L., Landschützer, P., Gruber, N., Lauvset, S. K.,and Stemmler, I.: Seasonal carbon dynamics in the near-global ocean. Global Biogeochemical Cycles, 34, e2020GB006571. doi:10.1029/2020GB006571, 2020.

Keppler, L., Landschützer, P., Lauvset, S.K., and Gruber, N.: Recent trends and variability in the oceanic storage of dissolved inorganic carbon. Global Biogeochemical Cycles, 37, e2022GB007677. Doi: 10.1029/2022GB007677, 2023.

Keraghel, M. A., Louanchi, F., Zerrouki, M., Kaci, M. A., Aït-Ameur, N., Labaste, M., Legoff, H., Taillandier, V., Harid, R., and Mortier, L.: Carbonate system properties and anthropogenic carbon inventory in the Algerian Basin during SOMBA cruise (2014): Acidification estimate, *Marine Chemistry*, https://doi.org/10.1016/j.marchem.2020.103783. 2020.

Key, R. M., Kozyr, A., Sabine, C. L., Lee, K., Wanninkhof, R., Bullister, J. L., Feely, R. A., Millero, F. J., Mordy, C., and Peng, T. H.: A global ocean carbon climatology: Results from Global Data Analysis Project (GLODAP), Global Biogeochemical Cycles, 18, GB4031, https://doi.org/10.1029/2004GB002247, 2004.

Key, R. M., Tanhua, T., Olsen, A., Hoppema, M., Jutterström, S., Schirnick, C., van Heuven, S., Kozyr, A., Lin, X., Velo, A., Wallace, D. W. R., and Mintrop, L.: The CARINA data synthesis project: introduction and overview, Earth Syst. Sci. Data, 2, 105–121, https://doi.org/10.5194/essd-2-105-2010, 2010.

Khatiwala, S., Tanhua, T., Mikaloff Fletcher, S., Gerber, M., Doney, S. C., Graven, H. D., Gruber, N., McKinley, G. A., Murata, A., Ríos, A. F., and Sabine, C. L.: Global ocean storage of anthropogenic carbon, Biogeosciences, 10, 2169-2191, https://doi.org/10.5194/bg-10-2169-2013, 2013.

Kitidis, V., Shutler, J. D., Ashton, I., Warren, M., Brown, I., Findlay, H., Hartman, S. E., Sanders, R., Humphreys, M., Kivimäe, C., Greenwood, N., Hull, T., Pearce, D., McGrath, T., Stewart, B. M., Walsham, P., McGovern, E., Bozec, Y., Gac, J.-P., van Heuven, S., Hoppema, M., Schuster, U., Johannessen, T., Omar, A., Lauvset, S. K., Skjelvan, I., Olsen, A., Steinhoff, T., Körtzinger, A., Becker, M., Lefèvre, N., Diverrès, D., Gkritzalis, T., Cattrijsse, A., Petersen, W., Voynova, Y., Chapron, B., Grouazel, A., Land, P. E., Sharples, J., and Nightingale, P. D.: Winter weather controls net influx of atmospheric CO_2 on the north-west European shelf. Sci Rep 9, 20153, doi:10.1038/s41598-019-56363-5. 2019.

Koffi U., Lefevre, N., Kouadio, G., and Boutin, J.: Surface CO2 parameters and air-sea CO2 fluxes distribution in the eastern equatorial Altantic Ocean. J. Marine Systems, doi:10.1016/j.jmarsys/2010.04.010. 2010.

Koffi, U., Georges, K., and Boutin, J.: Partial pressure (or fugacity) of carbon dioxide, dissolved inorganic carbon, alkalinity, temperature, salinity and other variables collected from Surface underway, discrete sample and profile observations using CTD, Carbon dioxide (CO2) gas analyzer and other instruments from ANTEA and L'ATALANTE in the Gulf of Guinea, North Atlantic Ocean and South Atlantic Ocean from 2005-06-09 to

2007-09-30 (NCEI Accession 0108086). [indicate subset used]. NOAA National Centers for Environmental Information. Dataset. https://doi.org/10.3334/cdiac/otg.egee1_6. Accessed [date]., 2013

Koseki, S., Tjiputra, J., Fransner, F. et al.: Disentangling the impact of Atlantic Niño on sea-air CO_2 flux. Nat Commun 14, 3649. https://doi.org/10.1038/s41467-023-38718-9, 2023.

Kwiatkowski, L., Torres, O., Bopp, L., Aumont, O., Chamberlain, M., Christian, J. R., Dunne, J. P., Gehlen, M., Ilyina, T., John, J. G., Lenton, A., Li, H., Lovenduski, N. S., Orr, J. C., Palmieri, J., Santana-Falcón, Y., Schwinger, J., Séférian, R., Stock, C. A., Tagliabue, A., Takano, Y., Tjiputra, J., Toyama, K., Tsujino, H., Watanabe, M., Yamamoto, A., Yool, A., and Ziehn, T.: Twenty-first century ocean warming, acidification, deoxygenation, and upper-ocean nutrient and primary production decline from CMIP6 model projections, Biogeosciences, 17, 3439–3470, https://doi.org/10.5194/bg-17-3439-2020, 2020.

Land, P. E., Findlay, H. S., Shutler, J. D., Ashton, I. G., Holding, T., Grouazel, A., Girard-Ardhuin, F., Reul, N., Piolle, J. F., Chapron, B., and Quilfen, Y.: Optimum satellite remote sensing of the marine carbonate system using empirical algorithms in the global ocean, the Greater Caribbean, the Amazon Plume and the Bay of Bengal. Remote Sensing of Environment, 235, p.111469, doi: 10.1016/j.rse.2019.111469, 2019.

Lauvset, S. K., Gruber, N., Landschützer, P., Olsen, A., and Tjiputra, J.: Trends and drivers in global surface ocean pH over the past 3 decades. Biogeosciences, 12, 1285-1298, doi:10.5194/bg-12-1285-2015, 2015

Lauvset, S. K., Carter, B. R., Perez, F. F., Jiang, L.-Q., Feely, R. A., Velo, A., and Olsen, A.: Processes Driving Global Interior Ocean pH Distribution, Global Biogeochem. Cycles, 34, e2019GB006 229, https://doi.org/10.1029/2019GB006229, 2020.

Lauvset, S. K., Lange, N., Tanhua, T., Bittig, H. C., Olsen, A., Kozyr, A., Álvarez, M., Becker, S., Brown, P. J., Carter, B. R., Cotrim da Cunha, L., Feely, R. A., van Heuven, S., Hoppema, M., Ishii, M., Jeansson, E., Jutterström, S., Jones, S. D., Karlsen, M. K., Lo Monaco, C., Michaelis, P., Murata, A., Pérez, F. F., Pfeil, B., Schirnick, C., Steinfeldt, R., Suzuki, T., Tilbrook, B., Velo, A., Wanninkhof, R., Woosley, R. J., and Key, R. M.: An updated version of the global interior ocean biogeochemical data product, GLODAPv2.2021, Earth Syst. Sci. Data, 13, 5565–5589, https://doi.org/10.5194/essd-13-5565-2021, 2021.

Lauvset, S. K., Lange, N., Tanhua, T., Bittig, H. C., Olsen, A., Kozyr, A., Alin, S., Álvarez, M., Azetsu-Scott, K., Barbero, L., Becker, S., Brown, P. J., Carter, B. R., da Cunha, L. C., Feely, R. A., Hoppema, M., Humphreys, M. P., Ishii, M., Jeansson, E., Jiang, L.-Q., Jones, S. D., Lo Monaco, C., Murata, A., Müller, J. D., Pérez, F. F., Pfeil, B., Schirnick, C., Steinfeldt, R., Suzuki, T., Tilbrook, B., Ulfsbo, A., Velo, A., Woosley, R. J., and Key, R. M.: GLODAPv2.2022: the latest version of the global interior ocean biogeochemical data product, Earth Syst. Sci. Data, 14, 5543–5572, https://doi.org/10.5194/essd-14-5543-2022, 2022.

Lebehot, A. D., Halloran, P. R., Watson, A. J., McNeall, D., Ford, D. A., Landschützer, P., Lauvset, S. K., and Schuster, U.: Reconciling Observation and Model Trends in North Atlantic Surface CO2, Global Biogeochem. Cy., 33, 1204–1222, https://doi.org/10.1029/2019GB006186, 2019.

Lee, K., Wanninkhof, R., Feely, R. A., Millero, F. J., and Peng, T.-H.: Global relationships of total inorganic carbon with temperature and nitrate in surface seawater, Global Biogeochem. Cy., 14, 979–994, https://doi.org/10.1029/1998GB001087, 2000.

Lee, K., Tong, L.T., Millero, F.J., Sabine, C.L., Dickson, A.G., Goyet, C., Park, G.H., Wanninkhof, R., Feely, R.A., and Key, R.M.: Global relationships of total alkalinity with salinity and temperature in surface waters of the world's oceans. *Geophys. Res. Lett.* 33, L19605. doi10.1029/2006GL027207. 2006.

Lefèvre, D.: MOOSE (ANTARES), https://doi.org/10.18142/233, 2010.

Lefèvre, N., Guillot, A., Beaumont, L, and Danguy, T.: Variability of fCO(2) in the Eastern Tropical Atlantic from a moored buoy. J. of Geophysical Research-Oceans, Volume: 113 Issue: C1, DOI: 10.1029/2007JC004146. 2008.

Lefèvre N., and Merlivat, L.: Carbon and oxygen net community production in the eastern tropical Atlantic estimated from a moored buoy. Global biogeochemical cycles, 26(1), 1-14. https://doi.org/10.1029/2010GB004018. 2012.

Lefèvre, N., Diverres, D., and Gallois, F.: Origin of CO2 undersaturation in the western tropical Atlantic: Tellus Series B Chemical and Physical Meteorology.Volume: 62 Issue: 5 Special Issue: SI Pages: 595-607 DOI: 10.1111/j.1600-0889.2010.00475.x, 2010.

Lefèvre N.: Carbon parameters along a zonal transect. SEANOE. https://doi.org/10.17882/58575, 2010.

Lefèvre, N., Veleda, D., Araujo, M., Caniaux, G.: Variability and trends of carbon parameters at a time series in the eastern tropical Atlantic. *Tellus B*, Co-Action Publishing, 68, pp.30305. 10.3402/tellusb.v68.30305. 2016.

Lefèvre, N., Mejia, C., Khvorostyanov, D., Beaumont, L., and Koffi, U.: Ocean Circulation Drives the Variability of the Carbon System in the Eastern Tropical Atlantic. Oceans, 2021, 2, 126–148. https://doi.org/10.3390/oceans2010008, 2021.

Lefèvre, N.: Discrete profile measurements of dissolved inorganic carbon, total alkalinity, temperature and salinity collected from R/V Antea French PIRATA cruise in Eastern Tropical Atlantic Ocean from 2009-07-10 to 2010-10-01 (NCEI Accession 0171193), 2018a.

Lefèvre, N.: Discrete surface measurements of dissolved inorganic carbon, total alkalinity, temperature and salinity collected from R/V Le Suroit French PIRATA cruise in Eastern Tropical Atlantic Ocean from 2011-05-03 to 2011-05-25 (NCEI Accession 0171197), 2018b.

Lefèvre, N.: Discrete profile measurements of dissolved inorganic carbon, total alkalinity, temperature and salinity collected from R/V Le Suroit French PIRATA cruise in Eastern Tropical Atlantic Ocean from 2012-03-21 to 2012-04-30 (NCEI Accession 0171195), 2018c.

Lefèvre, N.: Discrete surface measurements of dissolved inorganic carbon, total alkalinity, temperature and salinity collected from R/V Le Suroit French PIRATA cruise in Eastern Tropical Atlantic Ocean from 2013-05-11 to 2013-06-18 (NCEI Accession 0171189), 2018d.

Lefèvre, N.: Discrete profile measurements of dissolved inorganic carbon, total alkalinity, temperature and salinity collected from R/V Le Suroit French PIRATA cruise in Eastern Tropical Atlantic Ocean from 2014-04-10 to 2014-05-19 (NCEI Accession 0171194), 2018e.

Lefèvre, N.: Discrete surface measurements of dissolved inorganic carbon, total alkalinity, temperature and salinity collected from R/V Thalassa French PIRATA cruise in Eastern Tropical Atlantic Ocean from 2015-03-18 to 2015-04-15 (NCEI Accession 0171196), 2018f.

Lefèvre, N.: Discrete surface measurements of dissolved inorganic carbon, total alkalinity, temperature and salinity collected from R/V Thalassa French PIRATA cruise in Eastern Tropical Atlantic Ocean from 2016-03-08 to 2016-04-11 (NCEI Accession 0171190), 2018g.

Lefèvre, N.: Discrete surface measurements of dissolved inorganic carbon, total alkalinity, temperature and salinity collected from R/V Thalassa French PIRATA cruise in Eastern Tropical Atlantic Ocean from 2017-02-26 to 2017-03-30 (NCEI Accession 0171191), 2018h.

Le Quéré, C., Moriarty, R., Andrew, R. M., Canadell, J. G., Sitch, S., Korsbakken, J. I., Friedlingstein, P., Peters, G. P., Andres, R. J., Boden, T. A., Houghton, R. A., House, J. I., Keeling, R. F., Tans, P., Arneth, A., Bakker, D. C. E., Barbero, L., Bopp, L., Chang, J., Chevallier, F., Chini, L. P., Ciais, P., Fader, M., Feely, R. A., Gkritzalis, T., Harris, I., Hauck, J., Ilyina, T., Jain, A. K., Kato, E., Kitidis, V., Klein Goldewijk, K., Koven, C., Landschützer, P., Lauvset, S. K., Lefèvre, N., Lenton, A., Lima, I. D., Metzl, N., Millero, F., Munro, D. R.,

Murata, A., Nabel, J. E. M. S., Nakaoka, S., Nojiri, Y., O'Brien, K., Olsen, A., Ono, T., Pérez, F. F., Pfeil, B., Pierrot, D., Poulter, B., Rehder, G., Rödenbeck, C., Saito, S., Schuster, U., Schwinger, J., Séférian, R., Steinhoff, T., Stocker, B. D., Sutton, A. J., Takahashi, T., Tilbrook, B., van der Laan-Luijkx, I. T., van der Werf, G. R., van Heuven, S., Vandemark, D., Viovy, N., Wiltshire, A., Zaehle, S., and Zeng, N.: Global Carbon Budget 2015, Earth Syst. Sci. Data, 7, 349–396, https://doi.org/10.5194/essd-7-349-2015, 2015.

Lerner, P., Romanou, A., Kelley, M., Romanski, J., Ruedy, R., and Russell, G.: Drivers of Air-Sea CO_2 Flux Seasonality and its Long-Term Changes in the NASA-GISS model CMIP6 submission. Journal of Advances in Modeling Earth Systems, 13, e2019MS002028. Doi:10.1029/2019MS002028, 2021.

Leseurre, C., Lo Monaco, C., Reverdin, G., Metzl, N., Fin, J., Olafsdottir, S., and Racapé, V.: Ocean carbonate system variability in the North Atlantic Subpolar surface water (1993–2017), Biogeosciences, 17, 2553–2577, https://doi.org/10.5194/bg-17-2553-2020, 2020

Leseurre, C., Lo Monaco, C., Reverdin, G., Metzl, N., Fin, J., Mignon, C., and Benito, L.: Summer trends and drivers of sea surface fCO_2 and pH changes observed in the southern Indian Ocean over the last two decades (1998–2019), Biogeosciences, 19, 2599–2625, https://doi.org/10.5194/bg-19-2599-2022, 2022.

Lherminier, P., Mercier, H., Gourcuff, C., Alvarez, M., Bacon, S., and Kermabon, C.: Transports across the 2002 Greenland-Portugal OVIDE section and comparison with 1997. J. Geophys. Res., 112(C7), C07003, doi:10.1029/2006JC003716. 2007

Li, B. F., Watanabe, Y. W., Hosoda, S., Sato, K., and Nakano, Y.: Quasireal-time and high-resolution spatiotemporal distribution of ocean anthropogenic CO2. Geophysical Research Letters, 46, 4836–4843. https://doi.org/10.1029/2018GL081639, 2019.

Lo Monaco, C., Álvarez, M., Key, R. M., Lin, X., Tanhua, T., Tilbrook, B., Bakker, D. C. E., van Heuven, S., Hoppema, M., Metzl, N., Ríos, A. F., Sabine, C. L., and Velo, A.: Assessing the internal consistency of the CARINA database in the Indian sector of the Southern Ocean, Earth Syst. Sci. Data, 2, 51–70, https://doi.org/10.5194/essd-2-51-2010, 2010.

Lo Monaco, C., Metzl, N., Fin, J., and Tribollet, A.: Sea surface measurements of dissolved inorganic carbon (DIC) and total alkalinity (TALK), temperature and salinity during the R/V Marion-Dufresne cruise CLIM-EPARSES (EXPOCODE 35MV20190405) in the Indian Ocean and Mozambique Channel from 2019-04-04 to 2019-04-30. (NCEI Accession 0212218). [indicate subset used]. NOAA National Centers for Environmental Information. Dataset. https://doi.org/10.25921/26rw-w185. Accessed [date]. 2020.

Lo Monaco, C., Metzl, N., Fin, J., Mignon, C., Cuet, P., Douville, E., Gehlen, M., Trang Chau, T.T., and Tribollet, A.: Distribution and long-term change of the sea surface carbonate system in the Mozambique Channel (1963-2019), *Deep-Sea Research Part II*, https://doi.org/10.1016/j.dsr2.2021.104936 ,2021

Lombard, F., Bourdin, G. , Pesant, S., Agostini, S., Baudena, A., Boissin, E., Cassar, N., Clampitt, M., Conan, P., Da Silva, O., Dimier, C., Douville, E., Elineau, A., Fin, J., Flores, J.-M., Ghiglione, J.-F., Hume, B. C. C., Jalabert, L., John, S. G., Kelly, R. L., Koren, I., Lin, Y., Marie, D., McMinds, R., Mériguet, Z., Metzl, N., Paz-García, D. A., Luiza Pedrotti, M., Poulain, J., Pujo-Pay, M., Ras, J., Reverdin, G., Romac, S., Röttinger, E., Vardi, A., Voolstra, C. R., Moulin, C., Iwankow, G., Banaigs, B., Bowler, C., de Vargas, C., Forcioli, D., Furla, P., Galand, P. E., Gilson, E., Reynaud, S., Sunagawa, S., Thomas, O., Troublé, R., Vega Thurber, R., Wincker, P., Zoccola, D., Allemand, D., Planes, S., Boss, E., and Gorsky, G.: Open science resources from the Tara Pacific expedition across the surface ocean and coral reef ecosystems. Sci Data 10, 324 (2023). https://doi.org/10.1038/s41597-022-01757-w, 2022.

Lueker, T. J., Dickson, A. G., and Keeling, C. D.: Ocean pCO(2) calculated from dissolved inorganic carbon, alkalinity, and equations for K-1 and K-2: validation based on laboratory measurements of CO2 in gas and seawater at equilibrium. Marine Chemistry 70, 105-119. https://doi.org/10.1016/S0304-4203(00)00022-0, 2000.

Ma, D., Gregor, L., and Gruber, N: Four decades of trends and drivers of global surface ocean acidification. Global Biogeochemical Cycles, 37, e2023GB007765. 10.1029/2023GB007765, 2023.

Maier, C., Watremez, P., Taviani, M., Weinbauer, M. G, and Gattuso, J-P.: Calcification rates and the effect of ocean acidification on Mediterranean cold-water corals. *Proceedings of the Royal Society B-Biological Sciences,* 279(1734)**,** 1716-1723, doi:10.1098/rspb.2011.1763. 2012.

Margirier, F., Testor, P., Heslop, E. et al. : Abrupt warming and salinification of intermediate waters interplays with decline of deep convection in the Northwestern Mediterranean Sea. Sci Rep 10, 20923. 10.1038/s41598-020-77859-5, 2020.

Marrec, P., Cariou, T., Collin, E., Durand, A., Latimier, M., Macé, E., Morin, P., Raimund, S., Vernet, M., and Bozec, Y.: Seasonal and latitudinal variability of the CO_2 system in the western English Channel based on Voluntary Observing Ship (VOS) measurements. *Marine Chemistry, 155 (2013): 29–41*. 2013.

Marrec, P., Cariou, T., Latimier, M., Macé, E., Morin, P., Vernet, M., and Bozec, Y.: Spatio-temporal dynamics of biogeochemical processes and air–sea CO_2 fluxes in the Western English Channel based on two years of FerryBox deployment. Journal of Marine Systems, Special Issue: 5th FerryBox Workshop. 10.1016/j.jmarsys.2014.05.010. 2014.

Marrec, P., Cariou, T., Macé, E., Morin, P., Salt, L. A., Vernet, M., Taylor, B., Paxman, K., and Y. Bozec: Dynamics of air–sea CO_2 fluxes in the northwestern European shelf based on voluntary observing ship and satellite observations, *Biogeosciences*, 12, 5371-5391, doi:10.5194/bg-12-5371-2015. 2015

Marrec, P., and Bozec, Y.: Partial pressure (or fugacity) of carbon dioxide, dissolved inorganic carbon, alkalinity and salinity collected from Surface underway observations using Carbon dioxide (CO2) gas analyzer and other instruments from ARMORIQUE in the English Channel from 2012-04-25 to 2013-01-03 (NCEI Accession 0157472). Version 1.1. NOAA National Centers for Environmental Information. Dataset. doi:10.3334/CDIAC/OTG.COAST_FERRYBOX_ROSCOFF_PLYMOUTH_2012 [access date]. 2016a.

Marrec, P., and Bozec, Y.: Partial pressure (or fugacity) of carbon dioxide, dissolved inorganic carbon, alkalinity and salinity collected from Surface underway observations using Carbon dioxide (CO2) gas analyzer and other instruments from ARMORIQUE in the English Channel from 2013-03-15 to 2013-12-22 (NCEI Accession 0157444). Version 1.1. NOAA National Centers for Environmental Information. Dataset. doi:10.3334/CDIAC/OTG.COAST_FERRYBOX_ROSCOFF_PLYMOUTH_2013 [access date]. 2016b.

Marrec, P., and Bozec, Y.: Partial pressure (or fugacity) of carbon dioxide, dissolved inorganic carbon, alkalinity and salinity collected from surface underway observations using Carbon dioxide (CO2) gas analyzer and other instruments from ARMORIQUE in the English Channel from 2014-03-18 to 2014-10-09 (NCEI Accession 0163193). Version 1.1. NOAA National Centers for Environmental Information. Dataset. doi:10.3334/CDIAC/OTG.COAST_FERRYBOX_ROSCOFF_PLYMOUTH_2014 [access date]. 2017.

Mazloff, M. R., Verdy, A., Gille, S. T., Johnson, K. S., Cornuelle, B. D., and Sarmiento, J.: Southern Ocean acidification revealed by biogeochemical-Argo floats. *Journal of Geophysical Research: Oceans, 128,* e2022JC019530. https://doi.org/10.1029/2022JC019530, 2023.

McCulloch, M., Trotter, J., Montagna, P., Falter, J., Dunbar, R., Freiwald, A., Försterra, G., López Correa, M., Maier, C., Rüggeberg, A., and Taviani, M.: Resilience of cold-water scleractinian corals to ocean acidification: Boron isotopic systematics of pH and saturation state up-regulation. Geochimica et Cosmochimica Acta, Volume 87, 21-34. http://dx.doi.org/10.1016/j.gca.2012.03.027. 2012

McKinley, G. A., Fay, A. R., Takahashi, T., and Metzl, N.: Convergence of atmospheric and North Atlantic carbon dioxide trends on multidecadal timescales. Nature Geoscience. doi:10.1038/NGEO1193. 2011.

McKinley, G. A., Ritzer, A. L. and Lovenduski, N. S.: Mechanisms of northern North Atlantic biomass variability, Biogeosciences, 15(20), 6049–6066, doi:https://doi.org/10.5194/bg-15-6049-2018, 2018.

Meier, K. J. S., Beaufort, L., Heussner, S., and Ziveri, P.: The role of ocean acidification in Emiliania huxleyi coccolith thinning in the Mediterranean Sea, Biogeosciences, 11, 2857–2869, https://doi.org/10.5194/bg-11-2857-2014, 2014.

Mercier, H., Lherminier, P., Sarafanov, A., Gaillard, F., Daniault, N., Desbruyères, D., Falina, A., Ferron, B., Huck, T., and Thierry, V.: Variability of the meridional overturning circulation at the Greenland-Portugal Ovide section from 1993 to 2010. Progress in Oceanography, 132, 250-261, doi:10.1016/j.pocean.2013.11.001. 2015

Merlivat, L., Boutin, J., Antoine, D., Beaumont, L., Golbol, M., and Vellucci, V.: Increase of dissolved inorganic carbon and decrease in pH in near-surface waters in the Mediterranean Sea during the past two decades, Biogeosciences, 15, 5653-5662, https://doi.org/10.5194/bg-15-5653-2018, 2018.

Metzl, N., Brunet, C., Jabaud-Jan, A., Poisson, A., and Schauer, B.: Summer and winter air-sea CO2 fluxes in the Southern Ocean *Deep Sea Res I*, 53, 1548-1563, doi:10.1016/j.dsr.2006.07.006. 2006.

Metzl, N., Tilbrook, B., Bakker, D., Le Quéré, C., Doney, S., Feely, R., Hood M., and Dargaville, R.: Global Changes in Ocean Carbon: Variability and Vulnerability. Eos, Transactions of the American Geophysical Union 88 (28): 286-287. doi: 10.1029/2007EO280005, 2007.

Metzl, N., Corbière, A., Reverdin, G., Lenton, A., Takahashi, T., Olsen, A., Johannessen, T., Pierrot, D., Wanninkhof, R., Ólafsdóttir, S. R., Olafsson, J., and Ramonet, M.: Recent acceleration of the sea surface fCO2 growth rate in the North Atlantic subpolar gyre (1993-2008) revealed by winter observations, Global Biogeochem. Cycles, 24, GB4004, doi:10.1029/2009GB003658, 2010.

Metzl, N., and Lo Monaco, C.: OISO - OCÉAN INDIEN SERVICE D'OBSERVATION, https://doi.org/10.18142/228, 1998.

Metzl, N., Pierre, C., and Vangriesheim, A.: Hydrographic and Chemical measurements during the R/V L'Atalante BIOZAIRE III Cruise in the Atlantic Ocean (14 December, 2003 - 7 January 2004). http://cdiac.esd.ornl.gov/ftp/oceans/BIOZAIRE3. Carbon Dioxide Information Analysis Center, Oak Ridge National Laboratory, US Department of Energy, Oak Ridge, Tennessee. doi: 10.3334/CDIAC/OTG.BIOZAIRE3, 2016.

Metzl, N., Ferron, B. Lherminier, P. Sarthou, G. Thierry, V.: Discrete profile measurements of dissolved inorganic carbon (DIC), total alkalinity (TALK), temperature and salinity during the multiple ships Observatoire de la variabilité interannuelle et décennale en Atlantique Nord (OVIDE) project, OVIDE-2006, OVIDE-2008, OVIDE-2010, OVIDE-2012, OVIDE-2014 cruises in the North Atlantic Ocean from 2006-05-23 to 2014-06-30 (NCEI Accession 0177219). Version 1.1. NOAA National Centers for Environmental Information. Dataset. doi:10.25921/v0qt-ms48 [access date], 2018.

Metzl, N., Fin, J., Lo Monaco, C., et al.: A synthesis of total alkalinity and dissolved inorganic carbon measurements in the global ocean (1993-2022) SNAPO-CO2-V1 dataset. SEANOE. https://doi.org/10.17882/95414, 2023.

Mignot, A., Claustre, H., Cossarini, G., D'Ortenzio, F., Gutknecht, E., Lamouroux, J., Lazzari, P., Perruche, C., Salon, S., Sauzède, R., Taillandier, V., and Teruzzi, A.: Using machine learning and Biogeochemical-Argo (BGC-Argo) floats to assess biogeochemical models and optimize observing system design, Biogeosciences, 20, 1405–1422, https://doi.org/10.5194/bg-20-1405-2023, 2023.

Millero, F. J., Lee, K. and Roche, M.: Distribution of alkalinity in the surface waters of the major oceans. *Mar. Chem.* **60**, 111–130. https://doi.org/10.1016/S0304-4203(97)00084-4. 1998.

Mongwe, N. P., Vichi, M., and Monteiro, P. M. S: The seasonal cycle of *p*CO2 and CO2 fluxes in the Southern Ocean: Diagnosing anomalies in CMIP5 earth system models. *Biogeosciences*, *15*(9), 2851–2872. https://doi.org/10.5194/bg-15-2851-2018, 2018.

Mortier, L., Ait Ameur, N., and Taillandier, V. : SOMBA-GE-2014 cruise, RV Téthys II, https://doi.org/10.17600/14007500, 2014.

Moutin, T., and Bonnet, S. : OUTPACE cruise, RV L'Atalante, https://doi.org/10.17600/15000900, 2015.

Moutin, T., Wagener, T., Caffin, M., Fumenia, A., Gimenez, A., Baklouti, M., Bouruet-Aubertot, P., Pujo-Pay, M., Leblanc, K., Lefevre, D., Helias Nunige, S., Leblond, N., Grosso, O., and de Verneil, A.: Nutrient availability and the ultimate control of the biological carbon pump in the western tropical South Pacific Ocean, Biogeosciences, 15, 2961-2989, https://doi.org/10.5194/bg-15-2961-2018, 2018.

Newton, J.A., Feely, R. A., Jewett, E. B., Williamson, P. and Mathis, J.: Global Ocean Acidification Observing Network: Requirements and Governance Plan. Second Edition, GOA-ON, https://www.iaea.org/sites/default/files/18/06/goa-on-second-edition-2015.pdf, 2015.

Nykjaer, L.: Mediterranean Sea surface warming 1985-2006. Clim. Res. 39, 11–17. doi: 10.3354/cr00794, 2009.

Obernosterer, I.: MOBYDICK-THEMISTO cruise, RV Marion-Dufresne, https://doi.org/10.17600/18000403, 2018.

OCADS: Coastal Carbon Data, https://www.ncei.noaa.gov/access/ocean-carbon-acidification-data-system/oceans/coastal_carbon_data.html, 2023

Olafsson, J., Olafsdottir, S.R., Benoit-Cattin, A., Danielsen, M., Arnarson, T.S., and Takahashi, T.: Rate of Iceland Sea acidification from time series measurements. Biogeosciences 6, 2661–2668. https://doi.org/10.5194/bg-6-2661 2009, 2009.

Olivier, L., Boutin, J., Reverdin, G., Lefèvre, N., Landschützer, P., Speich, S., Karstensen, J., Labaste, M., Noisel, C., Ritschel, M., Steinhoff, T., and Wanninkhof, R.: Wintertime process study of the North Brazil Current rings reveals the region as a larger sink for CO_2 than expected, Biogeosciences, 19, 2969–2988, https://doi.org/10.5194/bg-19-2969-2022, 2022.

Olsen, A., Key, R. M., van Heuven, S., Lauvset, S. K., Velo, A., Lin, X., Schirnick, C., Kozyr, A., Tanhua, T., Hoppema, M., Jutterström, S., Steinfeldt, R., Jeansson, E., Ishii, M., Pérez, F. F., and Suzuki, T.: The Global Ocean Data Analysis Project version 2 (GLODAPv2) – an internally consistent data product for the world ocean, Earth Syst. Sci. Data, 8, 297–323, https://doi.org/10.5194/essd-8-297-2016, 2016.

Olsen, A., Lange, N., Key, R. M., Tanhua, T., Álvarez, M., Becker, S., Bittig, H. C., Carter, B. R., Cotrim da Cunha, L., Feely, R. A., van Heuven, S., Hoppema, M., Ishii, M., Jeansson, E., Jones, S. D., Jutterström, S., Karlsen, M. K., Kozyr, A., Lauvset, S. K., Lo Monaco, C., Murata, A., Pérez, F. F., Pfeil, B., Schirnick, C., Steinfeldt, R., Suzuki, T., Telszewski, M., Tilbrook, B., Velo, A., and Wanninkhof, R.: GLODAPv2.2019 – an update of GLODAPv2, Earth Syst. Sci. Data, 11, 1437–1461, https://doi.org/10.5194/essd-11-1437-2019, 2019.

Olsen, A., Lange, N., Key, R. M., Tanhua, T., Bittig, H. C., Kozyr, A., Álvarez, M., Azetsu-Scott, K., Becker, S., Brown, P. J., Carter, B. R., Cotrim da Cunha, L., Feely, R. A., van Heuven, S., Hoppema, M., Ishii, M., Jeansson, E., Jutterström, S., Landa, C. S., Lauvset, S. K., Michaelis, P., Murata, A., Pérez, F. F., Pfeil, B., Schirnick, C., Steinfeldt, R., Suzuki, T., Tilbrook, B., Velo, A., Wanninkhof, R., and Woosley, R. J.: An updated version of the global interior ocean biogeochemical data product, GLODAPv2.2020, Earth Syst. Sci. Data, 12, 3653–3678, https://doi.org/10.5194/essd-12-3653-2020, 2020.

Orr, J. C., Epitalon, J.-M., and Gattuso, J.-P.: Comparison of ten packages that compute ocean carbonate chemistry, *Biogeosciences*, 12(5), 1483–1510, doi:10.5194/bg-12-1483-2015, 2015.

Orr, J. C., Epitalon, J.-M., Dickson, A. G., and Gattuso, J.–P.: Routine uncertainty propagation for the marine carbon dioxide system, Marine Chemistry, Vol. 207, 84-107, doi:10.1016/j.marchem.2018.10.006., 2018.

Parard, G., Lefèvre, N., and Boutin, J.: Sea water fugacity of CO_2 at the PIRATA mooring at 6°S, 10°W. Tellus-B, DOI: 10.1111/j.1600-0889.2010.00503.x. 2010.

Pérez F. F., Vázquez-Rodríguez, M., Mercier, H., Velo, A., Lherminier, P. and Ríos, A. F.: Trends of anthropogenic CO_2 storage in North Atlantic water masses. Biogeosciences, 7, 1789-1807, doi:10.5194/bg-7-1789-2010, 2010.

Pérez, F. F., Mercier, H., Vazquez-Rodriguez, M., Lherminier, P., Velo, A., Pardo, P., Roson, G., and Rios, A.: Reconciling air-sea CO2 fluxes and anthropogenic CO2 budgets in a changing North Atlantic. Nature Geosciences, 6, 146-152, doi:10.1038/ngeo1680, 2013.

Pérez, F., Fontela, M., García-Ibáñez, M. et al. : Meridional overturning circulation conveys fast acidification to the deep Atlantic Ocean. Nature 554**,** 515–518. Doi: 10.1038/nature25493, 2018.

Pesant, S., Not, F., Picheral, M., Kandels-Lewis, S., Le Bescot, N., Gorsky, G., Iudicone, D., Karsenti, E., Speich, S., Troublé, R., Dimier, C., Searson, S., and Tara Oceans Consortium Coordinators: Open science resources for the discovery and analysis of Tara Oceans data. Scientific Data 2:150023. doi: 10.1038/sdata.2015.23, 2015.

Petrenko, A.: LATEX10 cruise, RV Téthys II, https://doi.org/10.17600/10450150, 2010.

Petrenko, A.A., Doglioli, A.M., Nencioli, F., Kersalé, M., Hu, Z., and d'Ovidio, F.: A review of the LATEX project: mesoscale to submesoscale processes in a coastal environment. Ocean Dynam., doi: 10.1007/s10236-017-1040-9, 2017.

Petton, S., Pouvreau, S., and Fleury, E. : ECOSCOPA network : high frequency environmental database. SEANOE. https://doi.org/10.17882/86131, 2023.

Pfeil, B., Olsen, A., Bakker, D. C. E., Hankin, S., Koyuk, H., Kozyr, A., Malczyk, J., Manke, A., Metzl, N., Sabine, C. L., Akl, J., Alin, S. R., Bates, N., Bellerby, R. G. J., Borges, A., Boutin, J., Brown, P. J., Cai, W.-J., Chavez, F. P., Chen, A., Cosca, C., Fassbender, A. J., Feely, R. A., González-Dávila, M., Goyet, C., Hales, B., Hardman-Mountford, N., Heinze, C., Hood, M., Hoppema, M., Hunt, C. W., Hydes, D., Ishii, M., Johannessen, T., Jones, S. D., Key, R. M., Körtzinger, A., Landschützer, P., Lauvset, S. K., Lefèvre, N., Lenton, A., Lourantou, A., Merlivat, L., Midorikawa, T., Mintrop, L., Miyazaki, C., Murata, A., Nakadate, A., Nakano, Y., Nakaoka, S., Nojiri, Y., Omar, A. M., Padin, X. A., Park, G.-H., Paterson, K., Perez, F. F., Pierrot, D., Poisson, A., Ríos, A. F., Santana-Casiano, J. M., Salisbury, J., Sarma, V. V. S. S., Schlitzer, R., Schneider, B., Schuster, U., Sieger, R., Skjelvan, I., Steinhoff, T., Suzuki, T., Takahashi, T., Tedesco, K., Telszewski, M., Thomas, H., Tilbrook, B., Tjiputra, J., Vandemark, D., Veness, T., Wanninkhof, R., Watson, A. J., Weiss, R., Wong, C. S., and Yoshikawa-Inoue, H.: A uniform, quality controlled Surface Ocean CO2 Atlas (SOCAT), Earth Syst. Sci. Data, 5, 125-143, doi:10.5194/essd-5-125-2013, 2013.

Picheral, M., Searson, S., Taillandier, V., Bricaud, A., Boss, E., Ras, J., Claustre, H., Ouhssain, M., Morin, P., Coppola, L., Gattuso, J.-P., Metzl, N., Thuillier, D., Gorsky, G., Tara Oceans Consortium, Coordinators; Tara Oceans Expedition, Participants: Vertical profiles of environmental parameters measured on discrete water samples collected with Niskin bottles during the Tara Oceans expedition 2009-2013. doi:10.1594/PANGAEA.836319, 2014.

Pilcher, D. J., Brody, S. R., Johnson, L., and Bronselaer, B.: Assessing the abilities of CMIP5 models to represent the seasonal cycle of surface ocean pCO2, J. Geophys. Res. Oceans, 120, 4625–4637, doi:10.1002/2015JC010759, 2015.

Poisson, A., Culkin, F., and Ridout, P.: Intercomparison of CO2 measurements. Deep Sea Research Part A. Oceanographic Research Papers, 37, 10, 1647-1650, https://doi.org/10.1016/0198-0149(90)90067-6, 1990.

Pujo-Pay, M., Durrieu de Madron, X., and Conan, P.: PERLE3 cruise, RV Pourquoi pas ?, https://doi.org/10.17600/18001342, 2020.

Pujo-Pay, M., Durrieu de Madron, X., and Conan, P.: PERLE4 cruise, RV L'Atalante, https://doi.org/10.17600/18001980, 2021.

Rabouille C.: AMOR-BFLUX cruise, RV Téthys II, https://doi.org/10.17600/15008700**,** 2015.

Racapé, V., Metzl, N., Pierre, C., Reverdin, G., Quay, P.D., and Olafsdottir, S. R.: The seasonal cycle of the $d13C_{DIC}$ in the North Atlantic Subpolar Gyre. Biogeosciences, 11, 6, 1683-1692, doi:10.5194/bg-11-1683-2014, 2014.

Revelle, R., and Suess, H. E.: Carbon dioxide exchange between atmosphere and ocean and the question of an increase of atmospheric CO2 during the past decades. Tellus 9, 18–27. doi:10.1111/j.2153-3490.1957.tb01849.x., 1957.

Reverdin, G.: STRASSE cruise, RV Thalassa, https://doi.org/10.17600/12040060, 2012.

Reverdin, G., Metzl, N., Olafsdottir, S., Racapé, V., Takahashi, T., Benetti, M., Valdimarsson, H., Benoit-Cattin, A., Danielsen, M., Fin, J., Naamar, A., Pierrot, D., Sullivan, K., Bringas, F., and Goni, G.: SURATLANT: a 1993–2017 surface sampling in the central part of the North Atlantic subpolar gyre, Earth Syst. Sci. Data, 10, 1901-1924, https://doi.org/10.5194/essd-10-1901-2018, 2018.

Reverdin, G., Metzl, N., Olafsdottir, S., Racapé, V., Takahashi, T., Benetti, M., Valdimarsson, H., Quay, P. D., Benoit-Cattin, A., Danielsen, M., Fin, J., Naamar, A., Pierrot, D., Sullivan, K., Bringas, F., and Goni, G.: SURATLANT: a surface dataset in the central part of the North Atlantic subpolar gyre. SEANOE. https://doi.org/10.17882/54517, 2022.

Ridame, C., Dekaezemacker, J., Guieu, C., Bonnet, S., L'Helguen, S., and Malien, F.: Contrasted Saharan dust events in LNLC environments: impact on nutrient dynamics and primary production, Biogeosciences, 11, 4783–4800, https://doi.org/10.5194/bg-11-4783-2014, 2014.

Robertson, J. E., Robinson, C., Turner, D. R., Holligan, P., Watson, A. J., Boyd, P., Fernandez, E., and Finch, M.: The impact of a coccolithophore bloom on oceanic carbon uptake in the northeast Atlantic during summer 1991, Deep Sea Res., Part I, 41(2), 297–314, 1994.

Rödenbeck, C., Keeling, R. F., Bakker, D. C. E., Metzl, N., Olsen, A., Sabine, C., and Heimann, M.: Global surface-ocean pCO2 and sea–air CO2 flux variability from an observation-driven ocean mixed-layer scheme, Ocean Sci., 9, 193–216, https://doi.org/10.5194/os-9-193-2013, 2013.

Rödenbeck, C., Bakker, D. C. E., Gruber, N., Iida, Y., Jacobson, A.R., Jones, S., Landschützer, P., Metzl, N., Nakaoka, S., Olsen, A., Park, G.-H., Peylin, P., Rodgers, K. B., Sasse, T. P., Schuster, U., Shutler, J. D., Valsala, V., Wanninkhof, R., Zeng, J. Data-based estimates of the ocean carbon sink variability – First results of the Surface Ocean pCO2 Mapping intercomparison (SOCOM). Biogeosciences 12: 7251-7278. doi:10.5194/bg-12-7251-2015, 2015.

Sabine, C. L., Feely, R. A., Gruber, N., Key, R. M., Lee, K., Bullister, J. L., Wanninkhof, R., Wong, C. S., Wallace, D. W. R., Tilbrook, B., Millero, F. J., Peng, T.-H., Kozyr, A., Ono, T., and Rios, A. F.: The Oceanic Sink for Anthropogenic CO_2, Science, 305, 367-371, https://doi.org/10.1126/science.1097403, 2004.

Sabine, C. L., Hankin, S., Koyuk, H., Bakker, D. C. E., Pfeil, B., Olsen, A., Metzl, N., Kozyr, A., Fassbender, A., Manke, A., Malczyk, J., Akl, J., Alin, S. R., Bellerby, R. G. J., Borges, A., Boutin, J., Brown, P. J., Cai, W.-J., Chavez, F. P., Chen, A., Cosca, C., Feely, R.A., González-Dávila, M., Goyet, C., Hardman-Mountford, N., Heinze, C., Hoppema, M., Hunt, C. W., Hydes, D., Ishii, M., Johannessen, T., Key, R. M., Körtzinger, A., Landschützer, P., Lauvset, S. K., Lefèvre, N., Lenton, A., Lourantou, A., Merlivat, L., Midorikawa, T., Mintrop, L., Miyazaki, C., Murata, A., Nakadate, A., Nakano, Y., Nakaoka, S., Nojiri, Y., Omar, A. M., Padin, X. A., Park, G.-H., Paterson, K., Perez, F. F., Pierrot, D., Poisson, A., Ríos, A. F., Salisbury, J., Santana-Casiano, J. M., Sarma, V. V. S. S., Schlitzer, R., Schneider, B., Schuster, U., Sieger, R., Skjelvan, I., Steinhoff, T., Suzuki, T., Takahashi, T., Tedesco, K., Telszewski, M., Thomas, H., Tilbrook, B., Vandemark, D., Veness, T., Watson, A. J., Weiss, R., Wong, C. S., and Yoshikawa-Inoue, H.: Surface Ocean CO2 Atlas (SOCAT) gridded data products, Earth Syst. Sci. Data, 5, 145-153, doi:10.5194/essd-5-145-2013, 2013.

Salt, L. A., Beaumont, L., Blain, S., Bucciarelli, E.,Grossteffan, E., Guillot, A., L'Helguen, S., Merlivat, L., Répécaud, M., Quéméner, L.,Rimmelin-Maury, P., Tréguer, P., and Bozec, Y.: The annual and seasonal variability of the carbonate system in the Bay of Brest (Northwest Atlantic Shelf, 2008–2014). Marine Chemistry, doi:10.1016/j.marchem.2016.09.003. 2016.

Sasse, T. P., McNeil, B. I., and Abramowitz, G.: A novel method for diagnosing seasonal to inter-annual surface ocean carbon dynamics from bottle data using neural networks, Biogeosciences, 10, 4319–4340, https://doi.org/10.5194/bg-10-4319-2013, 2013.

Sauzède, R., Claustre, H., Pasqueron de Fommervault, O., Bittig, H., Gattuso, J.-P., Legendre, L. and Johnson, K. S.: Estimates of water-column nutrients and carbonate system parameters in the global ocean: A novel approach based on neural networks. *Front. Mar. Sci.* 4:128. doi:10.3389/fmars.2017.00128, 2017.

Seelmann, K., Steinhoff, T., Aßmann, S., and Körtzinger, A.:. Enhance Ocean Carbon Observations: Successful Implementation of a Novel Autonomous Total Alkalinity Analyzer on a Ship of Opportunity. Front. Mar. Sci. 7:571301.doi: 10.3389/fmars.2020.571301, 2020.

Schlitzer, R.: Ocean Data View, Ocean Data View, http://odv.awi.de (last access: 13 March 2019), 2018.

Schneider, A., Wallace, D. W. R., and Körtzinger, A.: Alkalinity of the Mediterranean Sea, Geophys. Res. Lett., 34, L15608, doi:10.1029/2006GL028842, 2007.

Schuster, U., Watson, A.J., Bates, N., Corbière, A., Gonzalez-Davila, M., Metzl, N., Pierrot, D. and Santana-Casiano, M.: Trends in North Atlantic sea surface pCO2 from 1990 to 2006. Deep-Sea Res II, doi:10.1016/j.dsr2.2008.12.011, 2009.

Schuster, U., McKinley, G. A., Bates, N., Chevallier, F., Doney, S. C., Fay, A. R., González-Dávila, M., Gruber, N., Jones, S., Krijnen, J., Landschützer, P., Lefèvre, N., Manizza, M., Mathis, J., Metzl, N., Olsen, A., Rios, A. F., Rödenbeck, C., Santana-Casiano, J. M., Takahashi, T., Wanninkhof, R., and Watson, A. J.: An assessment of the Atlantic and Arctic sea–air CO2 fluxes, 1990–2009, Biogeosciences, 10, 607–627, https://doi.org/10.5194/bg-10-607-2013, 2013.

Sims, R. P., Holding, T. M., Land, P. E., Piolle, J.-F., Green, H. L., and Shutler, J. D.: OceanSODA-UNEXE: a multi-year gridded Amazon and Congo River outflow surface ocean carbonate system dataset, Earth Syst. Sci. Data, 15, 2499–2516, https://doi.org/10.5194/essd-15-2499-2023, 2023.

Skjelvan, I., Lauvset, S.K., Johannessen, T., et al.: Decadal trends in Ocean Acidification from the Ocean Weather Station M in the Norwegian Sea, Journal of Marine Systems, https://doi.org/10.1016/j.jmarsys.2022.103775, 2022.

Speich, S., and The Embarked Science Team: EUREC4A-OA. Cruise Report. 19 January – 19 February 2020. Vessel: L'ATALANTE. https://doi.org/10.13155/80129, 2021

Takahashi, T., Sutherland, S. C., Sweeney, C., Poisson, A., Metzl, N., Tilbrook, B., Bates, N., Wanninkhof, R., Feely, R. A., Sabine, C., Olafsson, J., and Nojiri, Y.: Global Sea-Air CO2 Flux Based on Climatological Surface Ocean pCO2, and Seasonal Biological and Temperature Effect. *Deep-Sea Res. II*, 49, 9-10, 1601-1622, https://doi.org/10.1016/S0967-0645(02)00003-6. 2002

Takahashi, T., Sutherland, S. C., Wanninkhof, R., Sweeney, C., Feely, R. A., Chipman, D. W., Hales, B., Friederich, G., Chavez, F., Sabine, C., Watson, A. J., Bakker, D. C., Schuster, U., Metzl, N., Yoshikawa-Inoue, H., Ishii, M., Midorikawa, T., Nojiri, Y., Körtzinger, A., Steinhoff, T., Hoppema, M., Olafsson, J., Arnarson, T. S., Tilbrook, B., Johannessen, T., Olsen, A., Bellerby, R., Wong, C., Delille, B., Bates, N., and de Baar, H. J.: Climatological mean and decadal change in surface ocean pCO2, and net sea air CO2 flux over the global oceans. Deep-Sea Res. II, 56 (8-10), 554–577, http://dx.doi.org/10.1016/j.dsr2.2008.12.009. 2009.

Takahashi, T., Sutherland, S. C., Chipman, D. W., Goddard, J. G., Ho, C., Newberger, T., Sweeney, C. and Munro, D. R.: Climatological distributions of pH, pCO2, total CO2, alkalinity, and CaCO3 saturation in the global surface ocean, and temporal changes at selected locations. Marine Chemistry, 164, 95–125, doi:10.1016/j.marchem.2014.06.004. 2014.

Tanhua, T., Pouliquen, S., Hausman, J., O'Brien, K., Bricher, P., de Bruin, T., Buck, J. J. H., Burger, E. F., Carval, T., Casey, K. S., Diggs, S., Giorgetti, A., Glaves, H., Harscoat, V., Kinkade, D., Muelbert, J. H., Novellino, A., Pfeil, B., Pulsifer, P. L., Van de Putte, A., Robinson, E., Schaap, D., Smirnov, A., Smith, N., Snowden, D., Spears, T., Stall, S., Tacoma, M., Thijsse, P., Tronstad, S., Vandenberghe, T., Wengren, M., Wyborn, L. and Zhao, Z.: Ocean FAIR Data Services. Front. Mar. Sci. 6:440. doi: 10.3389/fmars.2019.00440, 2019.

Tanhua, T., Lauvset, S.K., Lange, N. et al.: A vision for FAIR ocean data products. Commun Earth Environ 2, 136. https://doi.org/10.1038/s43247-021-00209-4, 2021

Testor, P., Bosse, A., and Coppola, L..: MOOSE-GE, https://doi.org/10.18142/235, 2010.

Testor, P.: DEWEX-MERMEX 2013 LEG1 cruise, RV Le Suroît, https://doi.org/10.17600/13020010, 2013.

Tilbrook, B., Jewett, E. B., DeGrandpre, M. D., Hernandez-Ayon, J. M., Feely, R. A., Gledhill, D. K., Hansson, L., Isensee, K., Kurz, M. L., Newton, J. A., Siedlecki, S. A., Chai, F., Dupont, S., Graco, M., Calvo, E., Greeley, D., Kapsenberg, L., Lebrec, M., Pelejero, C., Schoo, K. L., and Telszewski, M.: An Enhanced Ocean Acidification Observing Network: From People to Technology to Data Synthesis and Information Exchange. *Frontiers in Marine Science*, 6, 337, DOI:10.3389/fmars.2019.00337, 2019.

Touratier, F., Azouzi, L. and Goyet, C.: CFC-11, Δ14C and 3H tracers as a means to assess anthropogenic CO2 concentrations in the ocean. Tellus B, 59(2), 318–325, doi:10.1111/j.1600-0889.2006.00247.x, 2007.

Touratier, F., and Goyet, C.: Decadal evolution of anthropogenic CO_2 in the north western Mediterranean Sea from the mid-1990's to the mid-2000's. Deep Sea Research Part I.doi:10.1016/j.dsr.2009.05.015, 2009.

Touratier, F., Goyet, C., Houpert, L., Durrieu de Madron, X., Lefèvre, D., Stabholz, M., and Guglielmi, V.: Role of deep convection on anthropogenic CO_2 sequestration in the Gulf of Lions (northwestern Mediterranean Sea). Deep-Sea Research Part I. doi.org/10.1016/j.dsr.2016.04.003, 2016.

Turk, D., Dowd, M., Lauvset, S. K., Koelling, J., Alonso-Pérez, F. and Pérez, F. F.: Can Empirical Algorithms Successfully Estimate Aragonite Saturation State in the Subpolar North Atlantic? Front. Mar. Sci. 4:385. doi: 10.3389/fmars.2017.00385, 2017.

UNESCO: Intercomparison of total alkalinity and total inorganic carbon determinations in seawater. UNESCO Tech. Pap. Mar. Sci. 59., 1990

UNESCO: Reference materials for oceanic carbon dioxide measurements. UNESCO Tech. Pap. Mar. Sci. 60., 1991

United Nations. The Sustainable Development Goals 2020, 68pp. https://unstats.un.org/sdgs/report/2020/., 2020

Vangriesheim A., Pierre, C., Aminot, A., Metzl, N., Baurand, F., and Caprais, J.-C.: The influence of Congo river discharges in the surface and deep layers of the Gulf of Guinea. Deep-Sea Res. II, doi: 10.1016/j.dsr2.2009.04.002, 2009.

Vazquez-Rodriguez, M., Perez, F., Velo, A., Rios, A., and Mercier, H.: Observed acidification trends in the North Atlantic water masses. Biogeosciences, 9, 5217-5230, doi:10.5194/bg-9-5217-2012, 2012.

Velo, A., Perez, F. F., Brown, P., Tanhua, T., Schuster, U., and Key, R. M.: CARINA alkalinity data in the Atlantic Ocean, Earth Syst. Sci. Data, 1, 45–61, https://doi.org/10.5194/essd-1-45-2009, 2009.

von Schuckmann, K., Cheng, L., Palmer, M. D., Hansen, J., Tassone, C., Aich, V., Adusumilli, S., Beltrami, H., Boyer, T., Cuesta-Valero, F. J., Desbruyères, D., Domingues, C., García-García, A., Gentine, P., Gilson, J., Gorfer, M., Haimberger, L., Ishii, M., Johnson, G. C., Killick, R., King, B. A., Kirchengast, G., Kolodziejczyk, N., Lyman, J., Marzeion, B., Mayer, M., Monier, M., Monselesan, D. P., Purkey, S., Roemmich, D., Schweiger, A., Seneviratne, S. I., Shepherd, A., Slater, D. A., Steiner, A. K., Straneo, F., Timmermans, M.-L., and Wijffels, S. E.: Heat stored in the Earth system: where does the energy go?, Earth Syst. Sci. Data, 12, 2013–2041, https://doi.org/10.5194/essd-12-2013-2020, 2020.

von Schuckmann, K., Minière, A., Gues, F., Cuesta-Valero, F. J., Kirchengast, G., Adusumilli, S., Straneo, F., Ablain, M., Allan, R. P., Barker, P. M., Beltrami, H., Blazquez, A., Boyer, T., Cheng, L., Church, J., Desbruyeres, D., Dolman, H., Domingues, C. M., García-García, A., Giglio, D., Gilson, J. E., Gorfer, M., Haimberger, L., Hakuba, M. Z., Hendricks, S., Hosoda, S., Johnson, G. C., Killick, R., King, B., Kolodziejczyk, N., Korosov, A., Krinner, G., Kuusela, M., Landerer, F. W., Langer, M., Lavergne, T., Lawrence, I., Li, Y., Lyman, J., Marti, F., Marzeion, B., Mayer, M., MacDougall, A. H., McDougall, T., Monselesan, D. P., Nitzbon, J., Otosaka, I., Peng, J., Purkey, S., Roemmich, D., Sato, K., Sato, K., Savita, A., Schweiger, A., Shepherd, A., Seneviratne, S. I., Simons, L., Slater, D. A., Slater, T., Steiner, A. K., Suga, T., Szekely, T., Thiery, W., Timmermans, M.-L., Vanderkelen, I., Wjiffels, S. E., Wu, T., and Zemp, M.: Heat stored in the Earth system 1960–2020: where does the energy go?, Earth Syst. Sci. Data, 15, 1675–1709, https://doi.org/10.5194/essd-15-1675-2023, 2023.

Wagener, T., Metzl, N., Caffin, M., Fin, J., Helias Nunige, S., Lefevre, D., Lo Monaco, C., Rougier, G., and Moutin, T.: Carbonate system distribution, anthropogenic carbon and acidification in the western tropical South Pacific (OUTPACE 2015 transect), Biogeosciences, 15, 5221-5236, https://doi.org/10.5194/bg-15-5221-2018, 2018a.

Wagener, T., Metzl, N., Caffin, M., Fin, J., Helias Nunige, S., Lefevre, D., Lo Monaco, C., Rougier, G., and Moutin, T.: Discrete profile measurements of dissolved inorganic carbon (DIC), total alkalinity (TALK), temperature, salinity and other parameters during the R/V L'Atalante "Oligotrophy from Ultra-oligoTrophy PACific Experiment" (OUTPACE) cruise (EXPOCODE 35A320150218) in the South Pacific Ocean from 2015-02-18 to 2015-04-03 (NCEI Accession 0177706). Version 1.1. NOAA National Centers for Environmental Information. Dataset. doi:10.25921/wbkb-0q19 [access date], 2018b.

Walton, D. W. H., and Thomas, J.: Cruise Report - Antarctic Circumnavigation Expedition (ACE) 20th December 2016 - 19th March 2017 (1.0). Zenodo. https://doi.org/10.5281/zenodo.1443511, 2018.

Wanninkhof, R., Park, G.-H., Takahashi, T., Sweeney, C., Feely, R., Nojiri, Y,. Gruber, N., Doney, S. C., McKinley, G. A., Lenton, A., Le Quéré, C., Heinze, C., Schwinger, J., Graven, H., and Khatiwala, S.: Global ocean carbon uptake: magnitude, variability and trends, Biogeosciences, 10, 1983-2000, doi:10.5194/bg-10-1983-2013, 2013.

Watson, A. J., Schuster, U., Bakker, D .C. E., Bates, N., Corbiere, A., Gonzalez-Davila, M., Freidrich, T., Hauck, J., Heinze, C., Johannessen, T., Koertzinger, A., Metzl, N., Olafsson, J., Olsen, A., Oschlies, A., Padin, X., Pfeil, B., Rios, A., Santana-Casiano, M, Steinhoff, T., Telszewski, M., Wallace, D. W. R., and Wanninkhof, R.: Tracking the variable North Atlantic sink for atmospheric CO_2 , *Science* ,326, 1391, doi:10.1126/science.1177394. 2009.

Watson, A. J., Schuster, U., Shutler, J.D. et al.: Revised estimates of ocean-atmosphere CO_2 flux are consistent with ocean carbon inventory. Nat Commun 11**,** 4422, https://doi.org/10.1038/s41467-020-18203-3, 2020.

Williams, N. L., Juranek, L. W., Johnson, K. S., Feely, R. A., Riser, S. C., Talley, L. D., et al.: Empirical algorithms to estimate water column pH in the Southern Ocean. Geophysical Research Letters, 43, 3415–3422. https://doi.org/10.1002/2016GL068539, 2016.

Williams, N. L., Juranek, L. W., Feely, R. A., Johnson, K. S., Sarmiento, J. L., Talley, L. D., Dickson, A. G., Gray, A. R., Wanninkhof, R., Russell, J. L., Riser, S. C., and Takeshita, Y.: Calculating surface ocean pCO2 from biogeochemical Argo floats equipped with pH: An uncertainty analysis, Global Biogeochem. Cycles, 31, 591–604, doi:10.1002/2016GB005541., 2017.

Williams, N. L., Juranek, L. W., Feely, R. A., Russell, J. L., Johnson, K. S.,and Hales, B.: Assessment of the carbonate chemistry seasonal cycles in the Southern Ocean from persistent observational platforms. Journal of Geophysical Research: Oceans, 123. https://doi.org/10.1029/2017JC012917, 2018.

Wimart-Rousseau, C., Lajaunie-Salla, K., Marrec, P., Wagener, T., Raimbault,P., Lagadec, V., Lafont, M., Garcia, N., Diaz, F., Pinazo, C., Yohia, C., Garcia, F., Xueref-Remy,I., Blanc, P.-E., Armengaud, A., and Lefèvre, D.: Temporal variability of the carbonate system and air-sea CO_2 exchanges in a Mediterranean human-impacted coastal site. Estuarine, Coastal and Shelf Science. https://doi.org/10.1016/j.ecss.2020.106641, 2020a.

Wimart-Rousseau, C., Wagener, T., Raimbault, P., Lagadec, V., Lafont, M., Garcia, N., and Lefèvre, D.: Oceanic carbonate chemistry measurements from discret samples collected at the SOLEMIO station (Bay of Marseille - North western Mediterannean Sea) between 2016 and 2019. SEANOE. https://doi.org/10.17882/72356, 2020b.

Wimart-Rousseau, C., Wagener, T., Álvarez, M., Moutin, T., Fourrier, M., Coppola, L., Niclas-Chirurgien, L., Raimbault, P., D'Ortenzio, F., Durrieu de Madron, X., Taillandier, V., Dumas, F., Conan, P., Pujo-Pay, M. and Lefèvre, D.: Seasonal and Interannual Variability of the CO2 System in the Eastern Mediterranean Sea: A Case Study in the North Western Levantine Basin. Front. Mar. Sci. 8:649246. doi: 10.3389/fmars.2021.649246, 2021

WMO/GCOS, 2018: https://gcos.wmo.int/en/global-climate-indicators, 2018

Wu, Y., Hain, M. P., Humphreys, M. P., Hartman, S., and Tyrrell, T.: What drives the latitudinal gradient in open-ocean surface dissolved inorganic carbon concentration?, Biogeosciences, 16, 2661-2681, https://doi.org/10.5194/bg-16-2661-2019, 2019.